INSTITUTO NACIONAL DE PESQUISAS DA AMAZÔNIA – INPA
PROGRAMA DE PÓS-GRADUAÇÃO EM CIÊNCIAS DE FLORESTAS TROPICAIS

O *GREEN-UP* DA ESTAÇÃO SECA NA AMAZÔNIA CENTRAL É CONSISTENTE EM TRÊS DIFERENTES ESCALAS ESPACIAIS

NATHAN BORGES GONÇALVES

Manaus, Amazonas
Março, 2018

NATHAN BORGES GONÇALVES

O *GREEN-UP* DA ESTAÇÃO SECA NA AMAZÔNIA CENTRAL É CONSISTENTE EM TRÊS DIFERENTES ESCALAS ESPACIAIS

Orientador: Dr. Bruce Walker Nelson

Dissertação apresentada ao Instituto Nacional de Pesquisas da Amazônia, como parte dos requisitos para obtenção do título de Mestre em Ciências de Florestas Tropicais.

Manaus, Amazonas

Março, 2018

RELAÇÃO DA BANCA JULGADORA

ITEM	NOME	IES	Email
1	Paulo Maurício Lima de A. Graça	INPA	pmalencastro@gmail.com
2	Giordane Augusto Martins	INPA	giordanemartins@gmail.com
3	Rodrigo Augusto Ferreira Souza	UEA	souzaraf@gmail.com

INPA
INSTITUTO NACIONAL DE PESQUISAS DA AMAZÔNIA

MINISTÉRIO DA CIÊNCIA, TECNOLOGIA, INOVAÇÕES E COMUNICAÇÕES

BRASIL GOVERNO FEDERAL

PROGRAMA DE PÓS-GRADUAÇÃO EM CIÊNCIAS DE FLORESTAS TROPICAIS

DEFESA PÚBLICA DISSERTAÇÃO / PPG-CFT - INPA

Ata da Defesa Pública da Dissertação de Mestrado do (a) Sr (a) **NATHAN BORGES GONÇALVES** aluno (a) do Programa de Pós-Graduação *Stricto Sensu* em CIÊNCIAS DE FLORESTAS TROPICAIS, realizada no dia 16 de março de 2018.

Aos dezesseis dias do mês de março de 2018, às 09h00, no Auditório dos PPGs do ATU, CFT e ECO, Campus III, INPA-V8, realizou-se a Defesa Pública da Dissertação de Mestrado intitulada: "**O GREEN-UP DA ESTAÇÃO SECA NA AMAZÔNIA CENTRAL É CONSISTENTE EM TRÊS DIFERENTES ESCALAS ESPACIAIS**" em conformidade com o Artigo 68 do Regimento Interno do PPG-CFT e Artigo 52 do Regimento Geral da Pós-Graduação do Instituto Nacional de Pesquisas da Amazônia (MCTI-INPA) como parte final de seu trabalho para a obtenção do título de **MESTRE EM CIÊNCIAS DE FLORESTAS TROPICAIS**, área de concentração em Ciências de Florestas Tropicais. A **Banca Examinadora foi constituída pelos seguintes professores doutores: PAULO MAURÍCIO LIMA DE ALENCASTRO GRAÇA (INPA), GIORDANE AUGUSTO MARTINS (INPA), RODRIGO AUGUSTO FERREIRA SOUZA (UEA).** O (a) Presidente da Banca Examinadora, **Dr (a) Bruce Walker Nelson (Orientador/INPA)**, deu início à sessão convidando os senhores membros e o (a) Mestrando (a) a tomarem seus lugares e informou sobre os procedimentos a serem observados para o prosseguimento do exame. A palavra foi, então, facultada ao (à) Mestrando (a) que apresentou uma síntese do seu estudo e respondeu às perguntas formuladas pelos membros da Banca Examinadora. Depois da apresentação e arguição, a referida Banca Examinadora se reuniu e decidiu por

aprovar.

A sessão foi encerrada às 11h20e, para constar eu, Ana Serra, Assistente em C&T do INPA/PPG-CFT lavrei a presente Ata, que depois de lida e aprovada foi assinada pelo Presidente e membros da Banca Examinadora. Banca Examinadora:

Dr (a) PAULO MAURÍCIO LIMA DE A. GRAÇA	☒ Aprovado (a) ☐	Reprovado (a)
Dr (a) GIORDANE AUGUSTO MARTINS	☒ Aprovado (a) ☐	Reprovado (a)
Dr (a) RODRIGO AUGUSTO FERREIRA SOUZA	☒ Aprovado (a) ☐	Reprovado (a)

Dr (a) Bruce Walker Nelson
Presidente da Banca/Orientador

Joaquim dos Santos
Vice-coordenador do PPG CFT/INPA/MCTI
PO. N° 242/2017

INSTITUTO NACIONAL DE PESQUISAS DA AMAZÔNIA - INPA
PROGRAMA DE PÓS-GRADUAÇÃO EM CIÊNCIAS DE FLORESTAS TROPICAIS MESTRADO - DOUTORADO
Av. André Araújo, nº 2936 - Bairro: Petrópolis - Manaus/AM - CEP: 69057-375
Fone: (92) 3643-1838 Site: http://pg.inpa.gov.br - E-mails: cft@inpa.gov.br, ppgcft.secretaria@gmail.com

Gonçalves, Nathan Borges
O *green-up* da estação seca na Amazôna Central é consistente em três diferentes escalas espaciais/ Nathan Borges Gonçalves. --- Manaus: [s.n.], 2018.
49 f. : il. color.

Dissertação (Mestrado) --- INPA, Manaus, 2018.
Orientador : Bruce Walker Nelson.
Área de concentração: Ciências de Florestas Tropicais.

1. Fenologia. 2. Floresta tropical. 3. Demografia foliar. 4. *Green-up* da estação sfeca

CDD 581.5

Sinopse
Com o uso de câmeras fenológicas confirmou-se com êxito os padrões espectrais sazonais medidos por sensores orbitais remotos, contribuindo para um debate na literatura recente. Além disso, detectou-se um padrão anômalo no comportamento espectral e fenológico dos dosséis na Amazônia central após forte seca relacionada ao fenômeno El Niño.

Palavras-chave: Sensores orbitais, fenologia, LAI, El Niño, Amazônia central, seca

AGRADECIMENTOS

Ao meu orientador e grande mestre Dr. Bruce Walker Nelson

A CAPES pela bolsa de estudos.

Ao Programa de Pós-Graduação em Ciências de Florestas Tropicais do Instituto Nacional de Pesquisas da Amazônia (INPA) e todo o seu corpo docente e técnico.

Ao Convênio Max Planck, INPA, Ministério Federal Alemão de Educação e Pesquisa (BMBF contrato 01LB1001A), Ministério da Ciência, Tecnologia e Inovação (MCTI / FINEP contrato 01.11.01248.00), Universidade Estadual do Amazonas (UEA), FAPEAM, LBA/INPA e SDS/CEUC/ RDS-Uatumã, pelo projeto ATTO.

A Amanda, pelo companheirismo.

Aos meus grandes pais.

RESUMO

O *green-up* da estação seca em florestas de terra firme na Amazônia Central, detectado pelo Índice de Vegetação Melhorado (EVI) do sensor MODIS, tem sido objeto de recente controvérsia. A diminuição progressiva do ângulo zenital solar durante a estação seca reduz a quantidade de sombra no sub-pixel, causando um aumento na reflectância do NIR (Infravermelho próximo), e consequente aumento do EVI. A contaminação por nuvens também é fonte de artefatos, ainda mais em sensores com baixa resolução espacial como o MODIS. Para reduzir esses artefatos, utilizamos 16 anos de observações do produto MODIS-MAIAC (Multi-Angle Implementation of Atmospheric Correction), corrigidas para uma visão nadiral e 45º de ângulo zenital solar. Em seguida, obtivemos a reflectância de superfície para o sensor OLI LANDSAT 8 em dois locais da Amazônia Central, para fornecer corroboração independente da sazonalidade MODIS-MAIAC para o EVI, NIR e a Coordenada cromática verde (Gcc). Nós controlamos os efeitos de geometria de visada e iluminação no OLI usando datas com ângulos de elevação solar similares e comparando pixels com os mesmos ângulos de fase. Para três datas diferentes (fevereiro, maio, agosto) em um sítio, OLI e MODIS-MAIAC mostraram o mesmo ranking temporal para EVI, para NIR e para Gcc. Para duas datas (maio, dezembro) no segundo sítio -- tendo ângulos de elevação solar quase idênticos e ângulos de visada ao nadir -- as mudanças sazonais de EVI e NIR também foram corroboradas. Utilizamos, também, câmeras fenológicas instaladas em torres na Amazônia Central, 4 anos no ATTO (Amazon Tall Tower Observatory, 2 ° 8'36 "S e 59 ° 0'2" W) e 7 anos na torre k34 em Manaus (2 ° 36'33 "S, 60 ° 12'33" W), com intuito de obter Gcc na escala de copa e de paisagem e o LAI (Leaf Area index, com base na fração das copas com folhas). Obtivemos ainda a abundância das copas para determinadas classes de idade de suas folhas, com base na data do último flush foliar. Estas observações foram comparadas aos padrões sazonais de Gcc e EVI do MODIS-MAIAC centrados em cada torre. O Gcc do MODIS-MAIAC foi correlacionado positivamente com a variância entre copas do Gcc (R^2 = 0,68 e 0,53 na ATTO e k34, respectivamente). Em ambos os sítios, o EVI foi bem correlacionado com a abundância de folhas maduras, de 2-7 meses de idade (R^2 = 0,82 e 0,80, respectivamente), mas foi mal explicado pelo LAI (R^2 = 0,20 e 0,15, respectivamente), o que mostra que a demografia foliar e não quantidade de folhas controlam o EVI sazonal. No El Niño de 2015/16, observamos uma pequena anomalia de flush foliar em fevereiro-março e depois uma grande anomalia negativa em junho-julho, quando um pico de copas com flush ocorreria em anos com clima normal. Essas duas anomalias foram evidentes em ambos sítios, ATTO e K34, com o EVI e o Gcc do MODIS-MAIAC.

ABSTRACT

Dry season green-up of Central Amazon upland forest, as detected in the Enhanced Vegetation Index (EVI) of the Moderate resolution imaging spectro-radiometer (Modis) has been a subject of recent controversy. Progressive decrease in solar zenith angle during the dry season reduces sub-pixel shade content, causing artefactual increase in NIR reflectance, with consequent increase in EVI. Cloud contamination has also been difficult to detect and to filter given the large Modis pixel. To reduce these artifacts, we used 16y of 1km Modis-MAIAC (Multi-Angle Implementation of Atmospheric Correction) images, corrected to nadir view and 45^{o} solar zenith angles and having an improved cloud filter. We then obtained seasonal 30m Landsat 8 Operational Land Imager (OLI) surface reflectance at two Central Amazon sites, to provide independent corroboration of Modis-MAIAC seasonality for EVI, Near Infra-red (NIR) and Green chromatic coordinate (Gcc). We controlled for sun-sensor geometry effects in OLI by using dates with similar solar elevation angles and by comparing pixels with the same phase angles. For three different dates (Feb, May, Aug) at one site, OLI and Modis-MAIAC showed the same temporal ranking for EVI, for NIR and for Gcc. For two dates (May, Dec) at the second site -- having nearly identical solar elevation angles and near-nadir view angles -- EVI and NIR seasonal changes were also corroborated. We used Central Amazon tower-mounted RGB cameras, running for 4y at the Amazon Tall Tower (ATTO, 2° 8'36"S and 59°0’2"W) and 7y at the Manaus k34 tower (2°36'33"S, 60°12'33"W), to obtain landscape-scale and crown-scale Gcc, monthly Leaf Area Index (LAI, based on the fraction of upper canopy crowns that are leafy) and monthly leaf age class abundances by crown (based on time since last flush) in the camera view. These were compared to seasonal patterns of Gcc and EVI in 88 pixels of Modis-MAIAC centered on each tower. Modis-MAIAC Gcc was not always consistent with mean camera-derived Gcc but was positively correlated with the inter-crown variance of camera-derived Gcc (R^2 = 0.68 and 0.53 at ATTO and k34, respectively). At both sites, EVI was well correlated with the abundance of mature leaves 2-7 months old (R^2=0.82 and 0.80, respectively), but was poorly explained by LAI (R^2 = 0.20 and 0.15, respectively), which show that leaf demography and not leaf amount, is the main driver of seasonal EVI and of dry season green-up. After 6-7 months of lower-than-expected rainfall in 2015/16, we saw a small precocious positive flush anomaly in Feb-Mar, then a large negative flush anomaly in Jun-Jul, when a peak of flushing crowns would occur in normal climate years. These two flush anomalies were evident at both tower sites in Modis-MAIAC EVI and Gcc.

SUMÁRIO

LISTA DE FIGURAS

INTRODUÇÃO

Os efeitos da geometria de visada e iluminação na refletância são bem conhecidos para sensores orbitais e estão por trás de um recente debate sobre a detecção e magnitude dos fenômenos fenológicos em florestas de terra firme na Amazônia. Os padrões sazonais de *green-up* com base em imagens do sensor MODIS (Moderate resolution imaging spectro-radiometer) têm sido objeto de grande crítica (Galvão *et al*., 2011; Morton *et al*., 2014). Nos meses mais secos do ano de julho a novembro, às 10: 00-10: 30h quando as plataformas MODIS Terra e LANDSAT 8 cruzam a Amazônia Central, ângulos de elevação solar aumentam de 50 para cerca de 65 graus. Isso causa uma diminuição progressiva do conteúdo de sombra no sub-pixel e consequente aumento da refletância no infravermelho próximo (NIR) e no EVI (Enhanced vegetation index), causando um artefato (Galvão et al., 2011; Morton *et al*., 2014). De acordo com Morton *et al*. (2014), este artefato por si só explica o *green-up* da estação seca, contrastando com esforços anteriores que indicavam um aumento de cerca de 25% EVI do MODIS. Consistentes com medidas de fotossíntese em escala ecossistêmica (Huete *et al*., 2006).

Recentemente, um algoritmo que corrige artefatos relacionados a geometria de visada e iluminação, MAIAC (Multi-Angle Implementation of Atmospheric Correction), foi elaborado para o MODIS (Lyapustin *et al*., 2012). Esse algoritmo melhora a detecção e filtragem de nuvens e corrige as reflectâncias para ângulos fixos de visada e elevação solar, aplicando uma inversão empírica da função de distribuição de refletância bidirecional (BRDF), derivada de determinado número mínimo de observações para cada pixel dentro de um mosaico temporal de 16 dias. Aparentemente livre de artefatos de iluminação e visada, o MODIS-MAIAC, confirmou que cerca de metade da amplitude do padrão de *green-up*, não corrigido, da estação seca era real (Bi *et al*., 2015, Guan *et al*., 2015, Saleska *et al*., 2016). No entanto, esse é gerado com uma escala espacial de 1 km X 1km, deixando dúvidas quanto à remoção total de nuvens.

Para confirmar os padrões espectrais sazonais advindos do MODIS-MAIAC, a utilização de outros sensores com escala espacial mais fina e câmeras fenológicas são uma excelente alternativa. O OLI (Operational Land Imager) LANDSAT 8, com 30m X 30m de resolução espacial, poderia fornecer uma "ponte" entre as mudanças sazonais em escala de copa, relacionadas a idade e quantidade de folhas no dossel em um extremo espacial, e os dados espectrais do MODIS no outro extremo. No entanto, correções empíricas do BRDF são um desafio para o LANDSAT 8, uma vez que apenas uma combinação de ângulos de visualização e de iluminação por pixel é coletada em cada período de 16 dias. Soluções alternativas utilizam

parâmetros da anisotropia de MODIS ou sobreposições de órbitas vizinhas do LANDSAT (Danaher *et al*., 2001; Flood 2013), porém a baixa resolução temporal na estação chuvosa, época do ano na qual nuvens são abundantes, continua sendo um empecilho.

Uma simples solução aproveita o fato de que os ângulos de elevação solar na mesma hora do dia são repetidos até quatro vezes por ano perto do equador. Imagens LANDSAT com geometria de visada e iluminação idênticas ou muito similares podem estar disponíveis em datas selecionadas para diferentes estações do ano. Não sendo assim necessária uma correção BRDF para a comparação. Além disso, com um pixel de 30m X 30m, nuvens e névoas podem ser filtradas facilmente. Apesar da longa série histórica do LANDSAT, apenas com o aumento da resolução radiométrica do LANDSAT 8 pós-2013 foi possível um estudo fenológico desta natureza. Mesmo assim, imagens com ângulos de elevação solar similares ainda são bastante raras para a Amazônia Central e é muito improvável que coincidam com os sítios onde estão instaladas as câmeras fenológicas. No entanto, esses poucos locais possuem dados do MODIS-MAIAC. Portanto, essas imagens adquiridas com o OLI LANDSAT 8 sem nuvens que são incontestavelmente livres de artefatos de visada e iluminação podem ser usadas como uma confirmação independente de mudanças sazonais normais no EVI, conforme detectado pelo MODIS na mesma região.

Para explicar padrões espectrais vistos no MODIS-MAIAC, em termos de mudança na fenologia foliar de dossel, as câmeras fenológicas fornecem dados úteis com alta frequência temporal em uma escala local. Embora estas operem apenas na parte visível do espectro, fornecem dados sobre a idade e quantidade das folhas no dossel superior, que são conjuntamente responsáveis por uma grande parte do sinal do sensoriamento remoto óptico. As câmeras fenológicas já contribuíram para elucidar os principais fatores que controlam a sazonalidade da fotossíntese e da eficiência fotossintética (Wu *et al*., 2016). Vale ressaltar que a variação sazonal do LAI da Amazônia Central é pequena, variando de 5.5 a 6.2 (Wu *et al*., 2016), níveis em que a resposta espectral às mudanças de LAI está quase saturada. Por outro lado, a demografia foliar varia muito ao longo das estações, como mostrado pelas câmeras fenológicas (Lopes *et al*., 2016). Isso sugere que as diferenças sazonais no EVI são induzidas principalmente pela idade das folhas e menos pela mudança sazonal na quantidade. Esta inferência foi reforçada recentemente, por Wu *et al*. (2017), que predisseram o sinal do EVI como base na demografia foliar de dossel combinado a padrões espectrais de diferentes classes de idade de folhas. No entanto, uma comparação empírica dos atributos espectrais do dossel na escala das câmeras fenológicas (~ 1 m), LANDSAT (30m) e MODIS (1km) ainda não foi feita

e contribuirá para a compreensão da confiabilidade dos padrões espectrais sazonais detectados pelo MODIS e além dos mecanismos que controlam os padrões sazonais em escala foliar e de dossel.

Outro grande debate sobre a ecologia da floresta amazônica está relacionado aos efeitos interanuais da seca sobre a fenologia foliar. Durante a seca de 2005, Saleska *et al*. (2007) detectaram um *green-up* anômalo no MODIS EVI em toda a Amazônia, possivelmente impulsionado pelo aumento da disponibilidade de radiação solar. Esses resultados foram duramente criticados (Samantha *et al*., 2010) por conta da filtragem incompleta de nuvens. Além disso, algumas regiões apresentaram um período de anomalias negativas do EVI (*green-down*) na estação seca, uma tendência também relatada por Xu *et al*. (2011) durante a seca de 2010. A seca de 2015/2016, a mais forte registrada sobre o continente sul-americano (Erfanian *et al*., 2017), oferece uma ótima oportunidade para detectar eventuais alterações nos dosséis florestais com o uso de câmeras fenológicas e associar possíveis anomalias com índices de vegetação dos dados aprimorados do MODIS-MAIAC.

OBJETIVOS

Nossos objetivos se dividem em três grupos. Primeiro, nós testamos a predição que o OLI LANDSAT 8 irá corroborar os padrões sazonais detectados em três atributos espectrais do MODIS-MAIAC, todos os quais estão relacionados ao *green*-up da estação seca. Estes são: coordenadas verdes (Gcc), reflectância no infravermelho próximo (NIR) e EVI. Para este primeiro objetivo principal, escolhemos estrategicamente imagens do OLI LANDSAT 8 em datas que há um contraste sazonal claro nos indicadores do MODIS-MAIAC, porém também com diferenças mínimas nos ângulos de elevação solar.

Segundo, depois de reforçar a confiança no MODIS-MAIAC, comparamos os dados temporais do EVI do MODIS MAIAC com dados de câmeras de monitoramento fenológico em dois sítios na Amazônia Central. Utilizamos a abundância das copas em determinadas classes de idade e a quantidade de folhas (LAI), ambos estimados a partir de dados das câmeras. Nosso objetivo é determinar se a demografia foliar ou LAI explicam o MODIS-MAIAC EVI. Nós também procuramos um possível *driver*, relacionado à demografia foliar, do Gcc no MODIS-MAIAC.

Terceiro, estudamos anomalias relacionadas à seca de 2015/16 na demografia foliar em dois sítios para detectar se estas estão relacionadas a anomalias no MODIS-MAIAC Gcc e EVI.

Objetivo 1 – corroboração do OLI Landsat 8 com os padrões sazonais de Modis-MAIAC

Tomando como base um ano de dados fenológicos, Lopes *et al*. (2016) observaram que a maioria das copas no dossel superior fazem um *flush* foliar massivo uma vez por ano e a maioria desses eventos estão concentrados nos seis meses mais secos ano (junho a novembro). Durante 0-2 meses após o *flush*, as copas apresentaram alto verdor na região do visível, conforme representado pela coordenada verde (Gcc), que é a contribuição fracionada do canal ou banda verde em relação a soma das três bandas visíveis. Nos dados do orbitais, isso deve causar um pico de Gcc na estação seca. Isto deve ser seguido por picos de refletância de NIR e de EVI no final da estação seca até o início da chuvosa, uma vez que as folhas de 2-7 meses de idade tornam-se mais abundantes no dossel superior. Esta expectativa de EVI elevado em folhas de 2-7 meses de idade tem como base as diferentes respostas espectrais de fenofases distintas (Lopes *et al*., 2016; Wu *et al*., 2017).

Nós prevemos que tanto o OLI LANDSAT 8 quanto o MODIS-MAIAC mostrarão congruência entre padrões espectrais sazonais esperados pela demografia foliar. Especificamente, depois de controlar o ângulo de fase e selecionar imagens OLI em datas específicas que tenham ângulos de elevação solar similares, prevemos que:

Previsão 1. Landsat 8 OLI confirmará a sazonalidade MODIS-MAIAC do Gcc;

Previsão 2. Landsat 8 OLI confirmará a sazonalidade do EVI de MODIS-MAIAC e de seu principal driver, a reflectância do NIR;

Objetivo 2 –Sazonalidade do MODIS-MAIAC EVI impulsionada pela demografia foliar ou pela quantidade de folhas

Depois de obtermos a confirmação do OLI LANDSAT 8 para os padrões sazonais de MODIS-MAIAC para o Gcc, EVI e NIR, investigamos a congruência entre os padrões de demografia foliar de dossel vistos nas câmeras e os padrões espectrais vistos em dados MODIS-MAIAC. Primeiro perguntamos:

Q1. As medidas sazonais de Gcc do MODIS-MAIAC em dois sítios na Amazônia central são congruentes com a produção sazonal de novas folhas?

O monitoramento das câmeras fenológicas mostra que o número copas sem folhas atinge um pico na estação no meio da estação seca (~ agosto). Isso reduz ligeiramente a quantidade total de folhas no dossel (Wu *et al*., 2016). O EVI é sensível à quantidade de folhas no dossel Moura *et al*., 2016, Hilker *et al*., 2017), porém, o LAI muda pouco ao longo do ano, enquanto

a abundância de copas com folhas de 2-7 meses de idade varia bastante. Dessa modo, também perguntamos:

Q2.O Modis-MAIAC EVI em dois sítios na Amazônia Central está mais fortemente relacionado à demografia foliar de dossel do que a quantidade de folhas do dossel?

Objetivo 3. Controle da demografia foliar em anomalias do MODIS-MAIAC

Para esse objetivo perguntamos:

Q3. As anomalias com base na demografia foliar de dossel durante e após El Niño de 2015-2016 são detectáveis pelo EVI e Gcc de MODIS MAIAC?

Capítulo único

Gonçalves, N.B.; Lopes, A.P.; da Silva, R.D.; Nelson, B.W. Dry season green-up of Central Amazon forest is consistent across three spatial scales. Manuscrito em preparação para *Remote Sensing of Environment.*

Dry season green-up of Central Amazon forest is consistent across three spatial scales

Nathan B. Gonçalves, Aline P. Lopes[2,] Ricardo D. da Silva[2], Bruce W. Nelson[1]

[1] Brazilian National Institute for Amazon Research - INPA
{nathanborges, bnelsonbr }@gmail.com

[2] National institute for space research - INPE
alineplopes@gmail.com; ricds@hotmail.com

A short running title: Consistent central Amazon green-up across different scales

Keywords: tropical forest, dry season green-up, Enhanced Vegetation Index, phenocam, leaf demography, LAI, el ninõ, Central Amazon, Drought

Article type: Original Research

	Number of words
Abstract	438
Main text	7545

	Number
Figures	9
Tables	0

Corresponding author: Bruce Walker Nelson
bnelsonbr@gmail.com
2936 André Araújo Avenue, 69067-375, Manaus, AM, Brazil
Phone #: +55 92 3646 1906

ABSTRACT

Dry season green-up of Central Amazon upland forest, as detected in the Enhanced Vegetation Index (EVI) of the Moderate resolution imaging spectro-radiometer (Modis) has been a subject of recent controversy. Progressive decrease in solar zenith angle during the dry season reduces sub-pixel shade content, causing artefactual increase in NIR reflectance, with consequent increase in EVI. Cloud contamination has also been difficult to detect and to filter given the large Modis pixel. To reduce these artifacts, we used 16y of 1km Modis-MAIAC (Multi-Angle Implementation of Atmospheric Correction) images, corrected to nadir view and 45º solar zenith angles and having an improved cloud filter. We then obtained seasonal 30m Landsat 8 Operational Land Imager (OLI) surface reflectance at two Central Amazon sites, to provide independent corroboration of Modis-MAIAC seasonality for EVI, Near Infra-red (NIR) and Green chromatic coordinate (Gcc). We controlled for sun-sensor geometry effects in OLI by using dates with similar solar elevation angles and by comparing pixels with the same phase angles. For three different dates (Feb, May, Aug) at one site, OLI and Modis-MAIAC showed the same temporal ranking for EVI, for NIR and for Gcc. For two dates (May, Dec) at the second site -- having almost identical solar elevation angles and near-nadir view angles -- EVI and NIR seasonal changes were also corroborated. We used Central Amazon tower-mounted RGB cameras, running for 4y at the Amazon Tall Tower (ATTO, 2° 8'36"S and 59° 0’2"W) and 7y at the Manaus k34 tower (2°36'33"S, 60°12'33"W), to obtain landscape-scale and crown-scale Gcc, monthly Leaf Area Index (LAI, based on the fraction of upper canopy crowns that are leafy) and monthly leaf age class abundances in the camera view (based on time since leaf flushing, by crown). These were compared to seasonal patterns of Gcc and EVI in 88 pixels of Modis-MAIAC centered on each tower. Modis-MAIAC Gcc was not always consistent with mean camera-derived Gcc but was positively correlated with the intercrown variance of camera-derived Gcc (R^2 = 0.68 and 0.53 at ATTO and k34, respectively). At both sites EVI was well correlated with the abundance of mature leaves 2-7 months old (R^2=0.82 and 0.80, respectively, but was poorly explained by LAI (R^2 = 0.20 and 0.15, respectively).Therefore leaf demography, not leaf amount, is the main driver of seasonal EVI and dry season green-up. After 6-7 mo of lower-than-expected rainfall in 2015/16, we saw, in the tower mounted RGB cameras, a small precocious positive flush anomaly in Feb-Mar, then a large negative flush anomaly in Jun-July, when a peak of flushing crowns would occur in normal climate years. These two flush anomalies were evident at both tower sites in Modis-MAIAC EVI and Gcc.

INTRODUCTION

Sun-sensor geometry effects on reflectance are well known for orbital sensors and are behind a recent debate about the detection and magnitude of phenological phenomena in Amazon evergreen forests. Seasonal patterns of greenness based on MODIS images have been a subject of criticism (Galvão et al., 2011; Morton et al., 2014). At nadir view, solar zenith angles decrease by about 15 degrees during the drier months from July to November, when Modis Terra and Landsat 8 OLI platforms pass over the Central Amazon. This causes a progressive decrease in sub-pixel shade content and consequent increase in Near-infrared (NIR) reflectance and in Enhanced Vegetation Index (EVI), causing a greening artifact (Galvão et al., 2011; Morton et al., 2014). According to Morton et al. (2014) this artifact alone explains the dry season green-up, bringing into doubt an earlier report of 25% Modis EVI greening, consistent with ecosystem-scale photosynthesis measurements (Huete et al., 2006).

Recently, an angle corrected algorithm, MAIAC (multi-angle atmospheric correction) was elaborated for Modis (Lyapustin et al., 2012). This has improved cloud detection and filtering and corrects band reflectances to nadir view and fixed solar zenith angle by applying an empirical Bidirectional Reflectance Distribution Function (BRDF) inversion, derived from a minimum set of observations of each pixel within each 16-day temporal mosaic. Apparently free of sun-sensor artifacts, Modis-MAIAC confirmed that about half the amplitude of the uncorrected Modis dry-season green-up pattern was real (Bi et al., 2015, Guan et al., 2015, Saleska et al., 2016). However, Modis MAIAC is generated with a spatial scale of 1km, leaving doubts as to the full removal of clouds.

To confirm seasonal Modis-MAIAC derived seasonal spectral patterns, independent sensors with finer spatial scale are useful. The 30m Landsat 8 Operational Land Imager (OLI) provides a bridge between tower-based seasonal changes in crown color, leaf age mix and leaf amount at one spatial resolution extreme and Modis spectral data at the other extreme. However, empirical BRDF corrections at sub-seasonal frequency are a challenge for the Landsat 8 OLI sensor, as only one combination of view and illumination angles per pixel is collected in each 16-day time period. Workarounds use anisotropy parameters from Modis or from Landsat's neighboring orbit overlaps (Danaher et al., 2001; Flood 2013), but low temporal resolution in the cloudy wet season remains a problem.

One simple solution takes advantage of the fact that solar elevation angles at the fixed times of Landsat and of Modis overflight are repeated four times per year near the equator.

Landsat images having identical or very similar sun-sensor geometry are available at selected dates from different seasons of the year. No BRDF correction is required for their comparison, so these Landsat images can be used to validate modeled BRDF seasonal reflectance changes of Modis-MAIAC. With a 30m pixel, clouds and haze can also be more confidently filtered. Despite the long history of Landsat, only the high radiometric resolution of post-2013 Landsat 8 OLI is sufficiently precise for the comparisons of interest. Cloud-free areas in Landsat 8 image pairs having similar solar elevation angles at different seasons are still quite rare for the Central Amazon and are unlikely to coincide with tower camera sites. But these few places do have Modis-MAIAC data. Therefore, cloud-free Landsat 8 acquisitions date-pairs of that are unquestionably free of sun-sensor artifacts were used as an independent confirmation of normal seasonal changes in EVI as detected by Modis in the same region.

To explain spectral patterns seen by Modis-MAIAC, in terms of changing canopy leaf phenology, tower-mounted RGB cameras provide useful local-scale high-frequency data. While these operate only in the visible portion of the spectrum, RGB cameras provide data on upper canopy leaf age and leaf amount, which are jointly responsible for a large part of seasonal change in optical region canopy spectra. Tower-mounted RGB cameras have already contributed to elucidating the phenological drivers of seasonality in photosynthesis and photosynthetic efficiency at tower sites (Wu et al., 2016). Central Amazon LAI seasonal variation is small, ranging from 5.5 to 6.2 (Wu et al., 2016), levels at which spectral response to LAI changes are nearly saturated (Ponzoni, Shimabukuro & Kuplich, 2007). On the other hand, leaf demography varies greatly across seasons, as also shown by tower-mounted cameras (Lopes et al., 2016). This suggests that seasonal differences in EVI are induced mainly by leaf age and less by seasonal change in leaf amount. This inference has been strengthened recently by predicting seasonal changes in EVI using a radiative transfer model driven by changes in leaf amount and leaf age from camera data, combined with bare branch spectral and leaf spectra for different leaf age classes (Wu et al., 2017). Predicted and observed Modis-MAIAC EVI patterns were similar. Nonetheless, an empirical comparison of canopy spectral attributes at the scales of tower cameras (~1 m), Landsat (30m) and Modis (1km) has yet to be done and will contribute to our understanding of the reliability of the seasonal spectral patterns detected by Modis and the leaf-scale and canopy-scale drivers of these seasonal patterns.

Another subject of debate about Amazon forests is related to drought effects on inter-annual canopy phenology. During the 2005 drought, Saleska et al. (2007) detected anomalously

high greening in Modis EVI across Amazonia, possibly driven by increased availability of sunlight. These results were criticized (Samantha et al., 2010) for the incomplete cloud screening available in Modis collection 5. Furthermore, some regions presented a dry season browning, a tendency also reported by Xu et al. (2011) during the 2010 drought. The drought of 2015/2016, the strongest registered influence of El Niño over South American climate (Erfanian et al., 2017), provides an excellent opportunity to detect any changes in evergreen forests canopies as seen by tower-mounted cameras and associate these with possible anomalies in vegetation indexes using the improved Modis-MAIAC data now available.

OBJECTIVES

Our objectives fall into three groups. First, we predict that Landsat 8 OLI will corroborate the seasonal patterns detected in three spectral attributes from Modis-MAIAC, all of which are related to dry season green-up. These are Green chromatic coordinate (Gcc), Near Infra-red (NIR) reflectance and EVI. For this first main objective we use Landsat 8 OLI image dates strategically chosen to have clear seasonal contrast in the Modis-MAIAC indicators, but also having minimal differences in OLI solar elevation angles.

Second, having reinforced our confidence in Modis-MAIAC, we compare the fine-scale temporal data of this sensor's EVI in Modis pixels over two Central Amazon tower sites, to leaf-age class abundances and to leaf amount (LAI), both estimated from tower-mounted cameras. Our purpose is to determine whether leaf demography or LAI best explain Modis-MAIAC EVI. We compare the correlation coefficient between EVI and the abundance of a certain leaf age class and between EVI and LAI. To the same end, we use a radiative transfer model with fixed leaf spectra to ask if the observed seasonal LAI change can drive the observed seasonal EVI change. We also look for the camera-based leaf demography driver(s) of Gcc in Modis-MAIAC.

Third, we detect drought-related anomalies in leaf demography from camera data in 2015/16 at two tower sites to see if these are related to (and detectable as) anomalies in Modis-MAIAC Gcc and EVI.

Objective 1 – Landsat 8 OLI corroboration of Modis-MAIAC seasonal patterns

Based on one year of tower-camera data, Lopes et al. (2016) observed that most upper canopy crowns massively flush a new cohort of leaves once per year and most flushing events are concentrated in the six driest months (June to November at their study site). For 0-1 months after flushing, crowns had high visible "greenness", as represented by the Green chromatic coordinate (Gcc), the fractional contribution of the green channel or band to the sum of all three visible bands. In orbital sensor data, this should cause a Gcc peak in the mid dry season. This should be followed by peaks of NIR reflectance and of EVI in orbital sensors in the late dry to early wet season, as leaves of 2-7 months of age become more abundant in the upper canopy. This expectation of high EVI in leaves of 2-7 mo age is based on coupling RGB camera-based crown phenostages to the EVI of these same crown phenostages in high resolution QuickBird images (Lopes et al., 2016) and on seasonal patterns of a radiative transfer model driven by changes in canopy spectra with leaf age (Wu et al., 2017).

We predict that both Landsat 8 OLI and Modis-MAIAC will show congruence in these seasonal spectral patterns expected from (and driven by) leaf demography. Specifically, after controlling for phase angle and selecting OLI images on those specific dates that have similar solar elevation angles, we predict that:

Prediction 1. Landsat 8 OLI will confirm Modis-MAIAC seasonality of Gcc;

Prediction 2. Landsat 8 OLI will confirm Modis-MAIAC seasonality of EVI and of its main driver, NIR reflectance;

Objective 2 – Modis-MAIAC EVI seasonality driven by leaf demography or by leaf amount?

After obtaining confirmation from Landsat 8 OLI for the Modis-MAIAC seasonal patterns in Gcc, EVI and NIR using these few strategically selected dates, we then investigate congruence between year-round leaf demography patterns from RGB camera data and the year-round spectral patterns seen in MODIS-MAIAC data at the two tower camera sites. We first ask:

Q1. Are Modis-MAIAC seasonal Gcc measurements at Central Amazon tower sites congruent with seasonal new leaf production?

RGB camera monitoring shows that the number of leafless crowns reaches a peak in the mid dry season (~August). This reduces slightly the total leaf amount in the canopy (Wu et al. 2016). EVI is sensitive to canopy leaf amount (Brando et al., 2010, Moura et al., 2016, Hilker et al., 2017), but, LAI changes little over the year, whereas the abundance of crowns having leaves of 2-7 months of age varies greatly over the year. We therefore also ask:

Q2. Is Modis-MAIAC EVI at Central Amazon tower sites more strongly related to canopy leaf demography than to canopy leaf amount?

Objetive 3. Leaf demographic control over El Niño green-up anomalies

For this objective we ask:

Q3 Are camera-based anomalies in leaf demography during and after El Niño of 2015-2016 detectable in EVI and Gcc of Modis MAIAC?

MATERIAL AND METHODS

Landsat 8 OLI processing:

We used two methods to control sun-sensor geometry in Landsat 8 data, the second being more conservative than the first:

1- Controlling for the phase angle effect, while allowing minor difference (< 4^{o}) in solar elevation angle

To minimize the influence of sun-sensor geometry we searched for OLI images in the same Landsat scene with almost equal solar elevations. Solar elevation is a major concern, driving BRDF artifacts (Galvão et al., 2011; Morton et al., 2014). However, within a few degrees of the equator at the 10:00h Landsat passage time, it is possible to find up to four acquisition dates in the year for which solar elevations are similar. Differnces in view angle acros the image also contribute to BRDF artifacts. Therefore to represent sun-sensor geometry effects, we used the phase angle. The phase angle is the angle between the sun illumination vector of a pixel and sensor view vector of that same pixel (Bi et al., 2015). Phase angle of each pixel combines the main components of sun-sensor geometry effects on a pixel's reflectance into one variable (Maeda et al., 2015). The calculation is:

$Phase\ angle = ACOS$(cos(sensor view zen)×cos(Sun zen))+(SIN(sensor view zen)×SIN(Sun zen)*COS(Relative azim angle))

When the difference in solar elevation between two image acquisitions -- from different seasons that are to be compared -- is small at the scene center it is possible to find pixels with the same phase angle in distinct parts of the two images. Pixels with the same phase angle can have different solar azimuth angles, thus different amounts of topographic shade, but there should be no bias in this noise if topographic features have no preferred azimuthal orientations. In the Central Amazon, dates with small (< 4^o) difference in solar elevations and shared phase angles were chosen to coincide with strong seasonal differences in EVI and Gcc of local Modis-MAIAC and to also coincide with distinct phenological patterns found in tower RGB camera data (Lopes et al., 2016).

We were able to obtain three images with similar solar elevation angles for the Landsat scene 230/63, centered at 59.21^{o}W, 4.20^{o}S which is 160 km south-southeast of Manaus city. One image was from the mid wet season (11 Feb 2016) when tower-mounted cameras at Manaus-k34 and ATTO sites show very little leaf flushing or pre-flush leaf abscission (few bare crowns). Dark green leafy crowns predominate across the landscape. A second image was from the wet to dry season transition (25 May 2013), when old leaves are abundant and Leaf Area Index is approaching its minimum, as inferred from tower cameras (Wu et al., 2016). The third image was from the dry season (02 August 2015), when leafless crowns are most abundant and recently flushed crowns (0, 1 or 2 months since flush) are even more abundant. The image region selected for this method has an average dry season length of 2.9 months (from TRMM 3b43 v7), which is close to the dry season lengths at both the ATTO and Manaus k34 tower sites. Solar elevation angles at the scene center for the Wet, Wet-to-Dry and Dry season images were 57.85^o, 53.82^o and 53.87^o. Pixels with the same phase angles were compared.

2- Fixed nadir view and fixed solar elevation for NIR and EVI seasonal comparison

Controlling only for the phase angle, but allowing different solar elevations could conceivably cause bias in vegetation indices due to larger topographic shadows and larger crown shadows in the image with lower solar elevation (Morton et al., 2014, Galvão et al., 2016). Furthermore two sets of pixels may have the same phase angle but different relative azimuth angles, so that one date's pixel set is observed under forward-scattering geometry while

the other date is observed under backscatter geometry, which can affect vegetation indices (Moura et al., 2012). To eliminate these two problems and leave no doubt about seasonal patterns of EVI and NIR reflectance in the Landsat images, we used a more restrictive method that consists in comparing two images with nearly the same solar elevation at the scene center and also restricting the sensor view angle to $< 0.5^{o}$ off-nadir, ie. to a narrow strip of pixels close to the orbital track (Gonçalves et al., 2016). By limiting to a nadir view, the large interseasonal change in sun azimuth has no meaningful effect on relative azimuth angle. Pitfalls of sun-sensor geometry are fully resolved.

Finding cloud-free Landat 8 image areas that meet these more conservative conditions is challenging. We found a pair of images of the scene 230/61, centered at 1º 27'S and 58º 44'W (225 km NE of Manaus, and 90 km NNE of the ATTO tower) having solar elevation difference of only 0.6^{o}. The average dry season length is 3.4 months (from TRMM 3b43 v7). One image was from the late Wet season (15 May 2015) with 57.00 degrees solar elevation. The other was from the early Wet season (09 December 2015) with a scene center solar elevation of 57.56 degrees. These two Landsat dates are useful for confirming a very large expected difference in EVI and NIR (as seen in local Modis-MAIAC), but no strong difference in Gcc is expected, as seen in local tower camera data. We therefore extracted only EVI and NIR reflectance from Landsat and from Modis-MAIAC for these two dates. NIR is a proxy for EVI and is less affected by haze than other bands that comprise EVI. It is well known that NIR reflectance is the main control over EVI differences between Amazon forest pixels (Morton et al., 2014; Bi et al., 2015).

All five Landsat 8 images analyzed were in surface reflectance, as provided by the Landsat level 2 product. The data were downloaded from the Earth Explorer platform of the USGS. For all five dates we used only *terra firme* areas, i.e. excluding rivers, streams and floodplains. To this end we filtered all 30m Landsat pixels having less than 15m Vertical Distance to Channel Network (Conrad et al., 2015), an algorithm which uses 30m SRTM elevation data as the input. To minimize the effects of topographic shade, we accepted only those Landsat pixels with slope $< 4^{o}$. We masked all clouds and cloud shadows in Landsat using empirical thresholds of the SWIR1 band.

EVI was calculated as:

$$EVI = G.\frac{\rho NIR - \rho RED}{\rho NIR \ + \ C1 \cdot \rho red - C2 \cdot \rho blue \ + \ L)}$$

where ρx is the atmospherically corrected surface reflectance. The coefficients adopted were: L=1, C1=6, C2=7.5, and G=2.5 (Solano et al., 2010; Galvão et al., 2011).

Gcc was calculated as in phenological monitoring RGB cameras, but using reflectance instead of digital number (Sonnentag et al., 2012; Lopes et al., 2016):

$$Gcc = \frac{\rho Green}{\rho Green \ + \ \rho Red \ + \ \rho Blue}$$

where ρx is the atmospherically corrected surface reflectance.

All analyses were performed using the statistical and computational platform R and the raster package (R Development Core Team 2017; Hijmans 2016),

Modis MAIAC processing:

The MAIAC product was generated with empirical BRDF corrections to an apparent view zenith angle of 0º (nadir view) and an apparent solar zenith of 45º. and spatial resolution 1 km. MAIAC BRDF correction requires several cloud-free measurements of the same pixel in each window of 16 days, during which the sun-sensor geometry of that pixel must vary widely to provide the parameters for the inversion model (Lyapustin et al., 2012; Moura et al., 2012). Temporal resolution was 16 days Within each 16-day period canopy phenology of a pixel is therefore assumed to be constant and all differences in spectral reflectance are attributed to the BRDF effect which is being removed (Lyapustin et al., 2012).

In order to compare Modis MAIAC and Landsat 8, we obtained Modis observations that geographically match the areas of the two Landsat 8 scenes mentioned in the previous section. We used PRODES data (Valeriano et al., 2004) to mask deforestation in both Modis and Landsat. and 1 km resolution HAND data (Height Above Nearest Drainage) to mask rivers, streams and seasonally flooded areas (Rennó et al., 2008) in the Modis images. As with Landsat filtered by VCDN > 15m, we accepted only Modis pixels with HAND > 15m. The HAND algorithm is similar to the VDCN of Conrad et al. (2015), but the HAND facility presently does not process a full Landsat scene. We did not apply a slope restriction to the Modis data.

We calculated the spatial average of each spectral index or band over the usable Landsat scene area for each 16 day Modis MAIAC period in the time series from January 2001 to September 2016. For Landsat 8 we used five specific dates to represent the seasons, but for Modis-MAIAC, for our predictions (1) and (2), we used the 16y average of each 16d time window, as most years had limited data for the rainy season. Using 16y averages also reduced the short-term noise which is common in Modis data. We chose the five Modis-MAIAC 16d periods that matched the five dates on which Landsat images were collected. EVI and Gcc calculations for Modis-MAIAC were the same as for Landsat 8 data.

To answer our first and second questions, regarding congruence between Modis and tower-camera data, we used the mean values from two windows of 8x11 Modis-MAIAC pixels, one centered on the Manaus (k34) tower and one centered on the ATTO tower.

Phenocam leaf demography and digital processing:

We monitored the upper canopy leaf phenology from July 2013 to mid-2016 at the ATTO tower site (2° 8'36"S and 59° 0’2"W) with an RGB Stardot Netcam model XL 3MP camera, set to an interpolated resolution of 2048 x 1536 pixels. The camera was mounted 81 m above the ground and ~50 m above the forest canopy. Each of 270 upper canopy tree crowns was followed on a daily basis, always using images obtained under diffuse light (dense cloud shadow or overcast sky). At the k34 tower site (2°36'33"S, 60°12'33"W), we monitored from September 2010 to September 2016, with the same camera model, but mounted 51 above the ground. The image area at k34 included about 42 upper canopy crowns.

The age of each crown’s leaf cohort was determined by visually detecting the date of its abrupt leaf flush, which occurs in most trees once per year (Lopes et al. 2016). On a monthly basis we separated crowns that had flushed into three leaf age classes as suggested in Wu et al. (2016). However, we tried different transition ages to find the age class whose abundance best correlated with Modis-derived local EVI for the two tower sites. We calculated a camera-based LAI as a linear function (y=8.24*x-1.99) of the fraction of crowns that were leafy, following Wu et al. (2016), who calibrated this proxy using five years of monthly mean LAI obtained from the LAI-2000 instrument.

We compared the two correlations (EVI x leaf age class abundance and EVI x leaf amount) to see which was the more important driver of EVI seasonality. Furthermore, we ran

the ProSAIL radiative transfer model -- a combination of the PROSPECT leaf optical properties model and the SAIL canopy bidirectional reflectance model (Jacquemoud et al., 2009) -- to obtain the sensitivity of vegetation indices to the observed seasonal change in Leaf Area Index. Input leaf reflectance spectrum (and therefore the leaf age effect on EVI) was fixed in this model. If, under these input conditions, LAI is a weak driver of a vegetation index which has strong seasonality, then the seasonality of that index is likely to be driven mainly by the spectral changes of leafy canopies that are in turn associated with the abundance of different leaf age classes (Wu et al., 2017).

We also obtained the landscape-scale mean of Gcc and the inter-crown variance of Gcc for all analyzed crowns in the multi-year tower camera data for both sites. For digital analyses we follow methods in Lopes et al. (2016), using a separate Region of Interest (ROI) for each crown. However, we did not use image inter-calibration as their method removes the seasonal landscape scale change in Gcc and was meant only for detecting the large peaks and valleys in individual crown's Gcc timelines.

Of critical importance is the fact that we limited all digital analyses of tower camera data to images obtained under diffuse illumination. Direct light increases spectral contrast between crowns and this could affect the intercrown variance of Gcc, an artifact which we needed to eliminate. Diffusely lit images were obtainable even in the dry season because of the large number of daily images. RGB photos were captured every two minutes in a three-hour daily window, so that at least one image every three days was available under dense cloud shadow or densely overcast sky. It is also important to note that, if more frequent leakage of direct light through clouds during the dry season were driving seasonality of intercrown variance of Gcc (and of mean Gcc), then (1) the dry season intercrown variance would show a larger spread than the wet season and (2) some dry season images' Gcc variance would overlap with the wet season range of Gcc varance. Inspection of a single year of daily Gcc variance (Lopes et al, 2016, their Figure 6) shows that the images selected as diffusely lit pass both tests. Our expectation for our multi-year study (4y and 7y at two tower sites), is that mean Gcc and Gcc variance will both peak in the mid dry season when many scattered crowns have recently flushed ou new bright green leaves.

Anomalies of Modis MAIAC during El Niño:

For the two small windows of Modis pixels centered over each tower, we detected monthly anomalies in the 16y Modis MAIAC time series, from 2001 to 2016. Standardized anomalies for each month of each year for two vegetation indexes (EVI and Gcc) were calculated as:

Anomaly_my= (VI_my-Mean(VI_m))/(SD(VI_m))

where VI_my is the observed value for month m of year y, Mean (VI_m) is the 16y mean for month m over the period 2001-2016 and SD (VI_m) is the standard deviation of month m for the same 16y period. We considered a "significant" anomaly to be above or below two standard deviations from the 16y mean of a given month. We also investigated anomalies per trimester and bimester. We explored how anomalies during and after the 2015/16 El Niño in the Central Amazon might be linked to leaf demography changes at the Manaus (k34) and ATTO tower sites.

RESULTS

Prediction (1), seasonality of Gcc in Modis-MAIAC is confirmed by Landsat 8

Within the region of Landsat scene 230/63, 160 km SE of Manaus, we found strong seasonal change in Gcc for Modis-MAIAC, peaking in the mid-dry season (Fig 1B). For the three test dates shown as colored strips in Figure 1B, Landsat 8 corroborated Modis-MAIAC Gcc, showing the same temporal ordering of high-intermediate-low Gcc (Figure 2B). Amplitude changes were also similar. From the Wet to Dry dates of Landsat acquisitions, Modis MAIAC Gcc increased 4.6%±0.75 (95% CI of the mean) while Landsat 8 increased 3.7%±1.0 . Landsat 8 data show that season has a clear effect on Gcc when controlling for the phase angle ($p < 0.001$, $F(2,12611)=1182$) (Fig. 2). However, for the very narrow range of Landsat phase angles shared between the three image dates (35-37^{o}), phase angle control would not have been necessary, as it had no influence on the temporal separation of Gcc ($p = 0.9$, $F(1,12611) = 0.008$). We found a larger Landsat 8 Gcc increase from the Wet to Dry images, 5.9%±0.3; and a smaller increase from the Dry-wet transition to the Dry image, 2%±0.1.. This was also consistent with Modis-MAIAC.

Prediction (2), seasonality of NIR and EVI in Modis-MAIAC is confirmed by Landsat 8

Within the region of the same Landsat scene 160 km SE of Manaus, EVI of Modis-MAIAC reached a minimum in May which is the Wet-to-Dry transition and a peak in December, which is the early Wet season (Figure 1A). The three Landsat 8 EVI images corroborated this Modis-MAIAC seasonality, showing the same temporal ordering of high-intermediate-low EVI values as seen in Modis-MAIAC (Figure 2A). From the Wet-to-Dry transition date to the Wet date, increase in Modis-MAIAC EVI of 3.5%±1 appeared to be larger than that seen in Landsat (1.8%±0.75), a nearly significant difference.

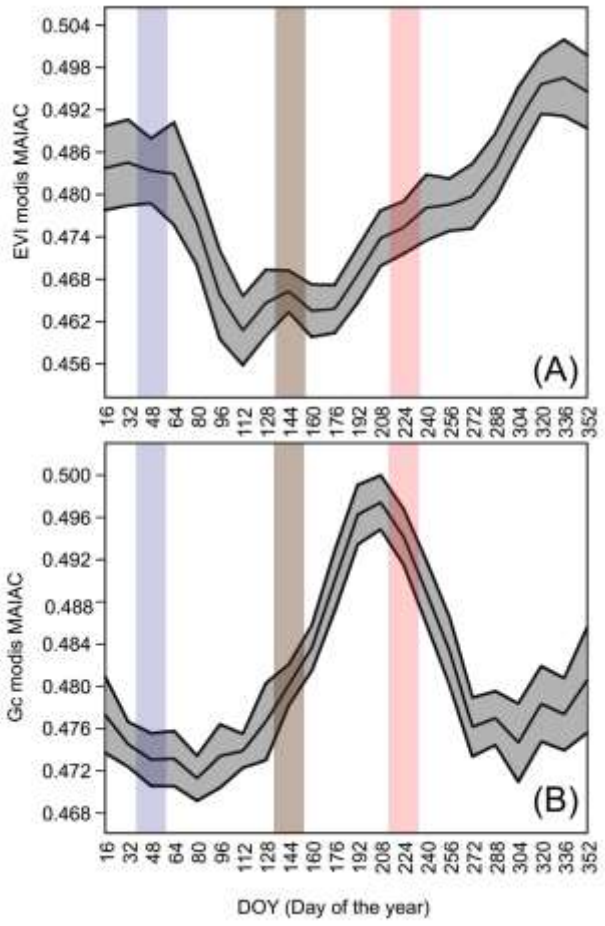

Fig. 1 Sixteen year mean Modis MAIAC EVI (A) and Gcc (B) for the upland area of Landsat scene 230/63. The colored strips indicate the three Modis 16d temporal mosaics that correspond to the Landsat image dates used for comparison to Modis. These are blue, brown and red, representing the Wet, Wet-to-Dry transition and Dry test dates, respectively.

Landsat 8 seasonal differences in EVI were significant when controlling for the effect of small changes (range = 2º) in phase angle ($p < 0.001$, $F(2,12611) = 289$)). Increasing phase

angle depressed EVI ($p < 0.001$, $F(1,12611) = 74.4$)). This is as expected since pixels with larger phase angles tend to have more sub-pixel shade. The largest increase in EVI was found from the Wet-to Dry transition towards Wet image date, 6.9±0.4%. A smaller increase of EVI occurred from the Wet-dry transition towards Dry image 2.7±0.2%. This was also consistent with Modis-MAIAC (Fig 1A).

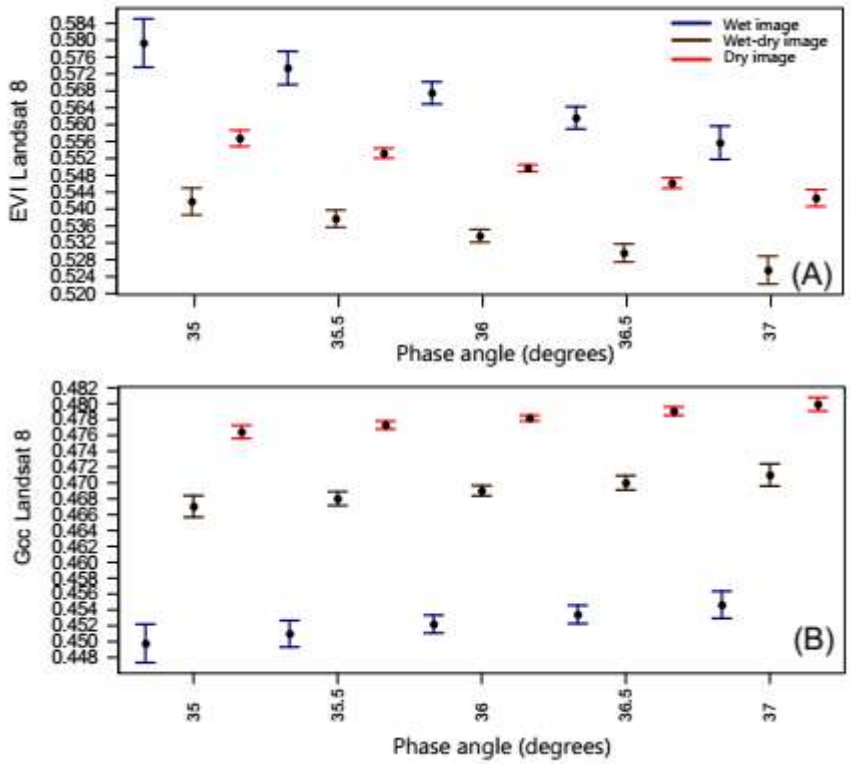

Fig 2. EVI (A) and Gcc (B) from Landsat 8 for upland forests in scene 230/63, controlling for phase angle (X-axis) and allowing slightly different solar elevation and view angles. Error bars are 95% CI of the mean for each of five phase angle bins for each Landsat date. Blue, brown and red colors represent Wet, Wet-to-Dry and Dry season image dates, as in Figure 1

For the Landsat 8 image pair from scene 230/61, 225 km NE of Manaus, for which solar elevation angles were nearly identical and spectral comparisons were restricted to < 0.5º off-nadir view, we found an increase of 8.4% ± 0.13 for EVI from May to December. This was again consistent with expectations from Modis-MAIAC (Fig. S1 in Supplementary data). Driving this EVI behavior was an increase of 13% ± 0.16) in Landsat NIR reflectance from May to December (Fig.3).

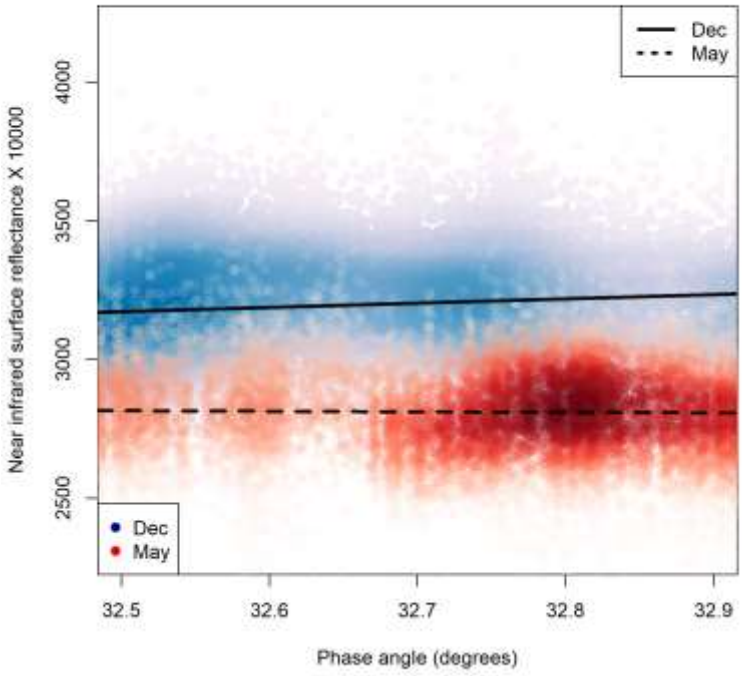

Fig. 3. Seasonal increase in near-nadir NIR reflectance in Landsat 8 scene 230/61 from May 2015 (red) to December 2015 (blue), two images with nearly identical solar elevation angles. Lines are linear regression fits.

Q1. Are Modis-MAIAC seasonal Gcc measurements congruent with seasonal new leaf production in the Central Amazon?

We use inter-crown variance as a proxy for seasonal leaf flush in the camera data. Confirming our expectation, intercrown variance of Gcc peaks in the early dry season at both tower sites, probably a consequence of the large number of recently flushed crowns (high Gcc) interspersed with a large number of pre-flush abscising crowns (low Gcc). As shown by Fig 6, seasonal Modis-MAIAC Gcc closely followed the tower camera based inter-crown variance of Gcc at both ATTO (R^2 = 0.68, $p < 0.001$) and at Manaus k34 (R^2 = 0.53, $p < 0.001$), after applying a one-month forward shift to the camera data.

Q2. Which best explains the seasonality of Modis MAIAC EVI in the Central Amazon: total canopy leaf amount or upper canopy leaf demography?

Seasonal Modis MAIAC EVI was strongly correlated with the abundance of the 'mature' (Fig. 4) leaf class in the upper canopy, of 2-7 months age, at both ATTO (R^2 = 0.82, $p < 0.001$) and Manaus k34 (R^2 =0.80, $p < 0.001$). Modis MAIAC EVI was also highly correlated with mean Gcc of all upper canopy tree crowns (Fig. 5A) when this latter variable was shifted one month forward (R^2=0.72, $p < 0.001$). Total LAI, on the other hand, was a poor predictor of EVI at ATTO (R^2 = 0.20, p = 0.018) and at Manaus – k34 (R^2 = 0.15, p = 0.002)

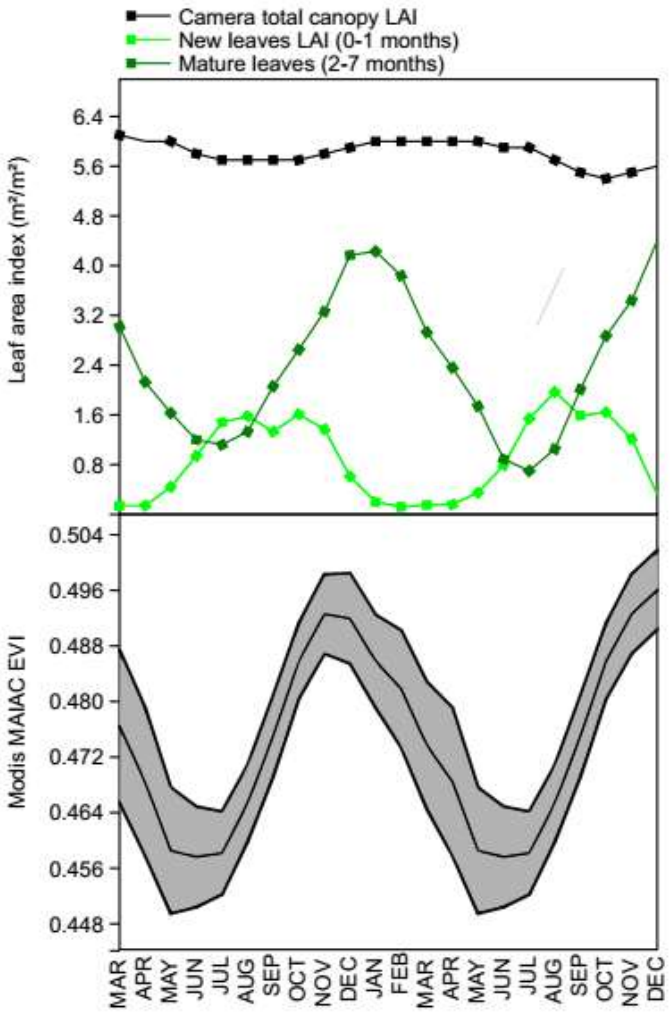

Fig. 4. A) Camera-based total canopy Leaf area index (LAI) and LAI in two different ages groups, new leaves (0 to 1 month of age) and mature leaves (2 to 7 months of age) for the ATTO site. B) Seasonal Modis MAIAC EVI from March of 2014 to December 2015 at ATTO site.

Q3. Are camera-based anomalies in leaf demography during and after the El Niño of 2015-2016 detectable in EVI and Gcc of Modis MAIAC?

At the two tower sites, Manaus k34 and ATTO, lower-than-normal rainfall associated with a strong El Niño began in August of 2015 and ended in mid-March of 2016. Both sites presented large positive anomalies (>2.5 SD) for Modis-MAIAC EVI in the second trimester of 2016 (Apr-May-Jun) (Fig. 5B,C). In the same period, we detected in the tower camera data an anomalously high fraction of crowns with leaves 2-4 months age (Fig 5B,C), an age at which EVI at the individual leaf scale reaches its maximum (Yang et al. 2014, Lopes et al. 2016). This peak of 2-4 mo old leaves was preceded by a small anomalous leaf flush in February and March of 2016 at both sites. (However, in raw numbers, there were six flushing crowns in March 2016 at k34 and 12 flushing crowns in March at ATTO.) An unusual paucity of flushing crowns occurred in the second trimester of 2016, compared with this same trimester in prior non-drought years as detected by the tower cameras (Fig 6 B,C). The El Niño seems to have been associated with a small advanced flush (Feb-Mar, 2016) and a larger "missing" flush two to three months later. The missing flush is evident as an unusually low fraction of flushing crowns in the trimester Apr-May-Jun of 2016, relative to prior years for this same trimester at both towers (Fig 6 B, C). These low post El Niño flush rates at both sites appear as large negative anomalies in local Modis MAIAC Gcc(Fig 6 B, C).

For the 2.5y starting Feb 2014 mean camera Gcc across all upper canopy crowns at ATTO, when shifted forward by one month, closely tracked EVI from Modis-MAIAC, with R^2=0.72 (Fig 5A). One-month forward-shifted mean camera Gcc was also correlated with the cohort of mature leaves of 2-4 months age (R^2=0.60).

From Aug 2013 to Nov 2015, i.e., prior to any El Niño effects, the intercrown variance of Gcc from the cameras closely tracked Modis-MAIAC Gcc (Fig 6A). The accumulation of recently flushed crowns, which have high Gcc, apparently overwhelms the signal of the more ephemeral pre-flush deciduous crowns, which have low Gcc (Lopes et al. 2016). The mixture of these two phenostages is seem mostly in the dry months and causes the high intercrown variance from camera data at that time of year, contrasting with the rainy season, when most crowns are the same dark leafy green (intermediate Gcc values), leading to low intercrown variance of Gcc. From November 2015 to July 2016, (i.e., during and after the El Niño) camera-based intercrown variance behaved normally, dropping in the rainy season and rising in the dry months, but Modis-MAIAC Gcc remained moderately high and stable through the El Nino rainy

season and into the following dry season. Non-regularity of seasonal Modis-MAIAC Gcc was seen in earlier years as well (not shown).

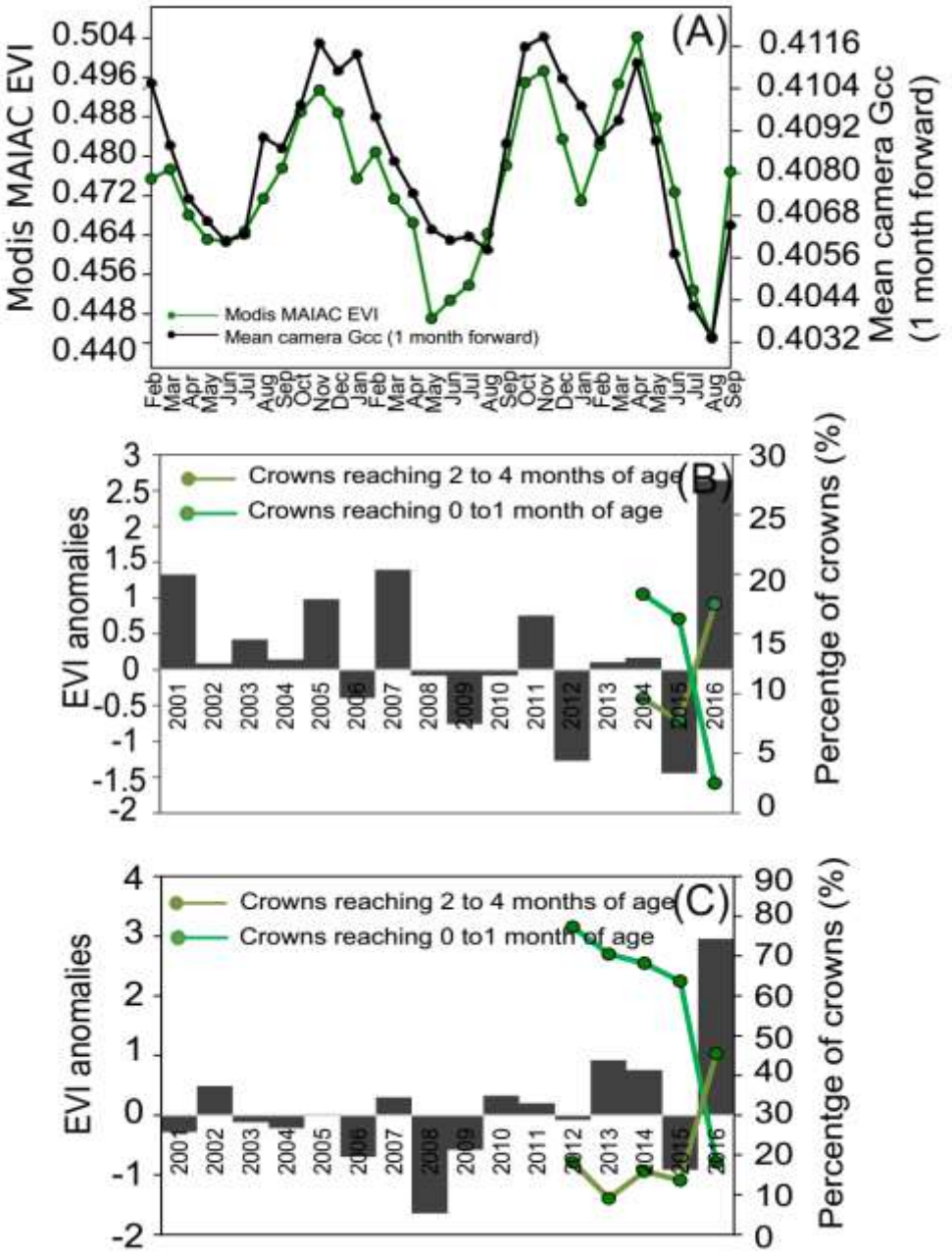

Fig 5. A) Modis MAIAC EVI and Mean Camera Gcc at ATTO site from February 2014 to September 2016. Mean camera Gcc is shifted one month forward. B) Modis-MAIAC EVI anomalies at the ATTO site for the second trimester of each year (Apr-May-Jun) and the percentage of crowns reaching 0-1 month age (recently flushed) and 2-4 months age, also in the second trimester of each year. C) Modis-

MAIAC EVI anomalies for the second trimester of each year at the Manaus-k34 site and the percentage of crowns reaching 0-1months and 2-4 months of age in the second trimester of each year. “Percentage of crowns” is always with respect to the total number of crowns that flushed in a year; non-flushing crowns are excluded from the calculation as their leaf demography cannot be inferred.

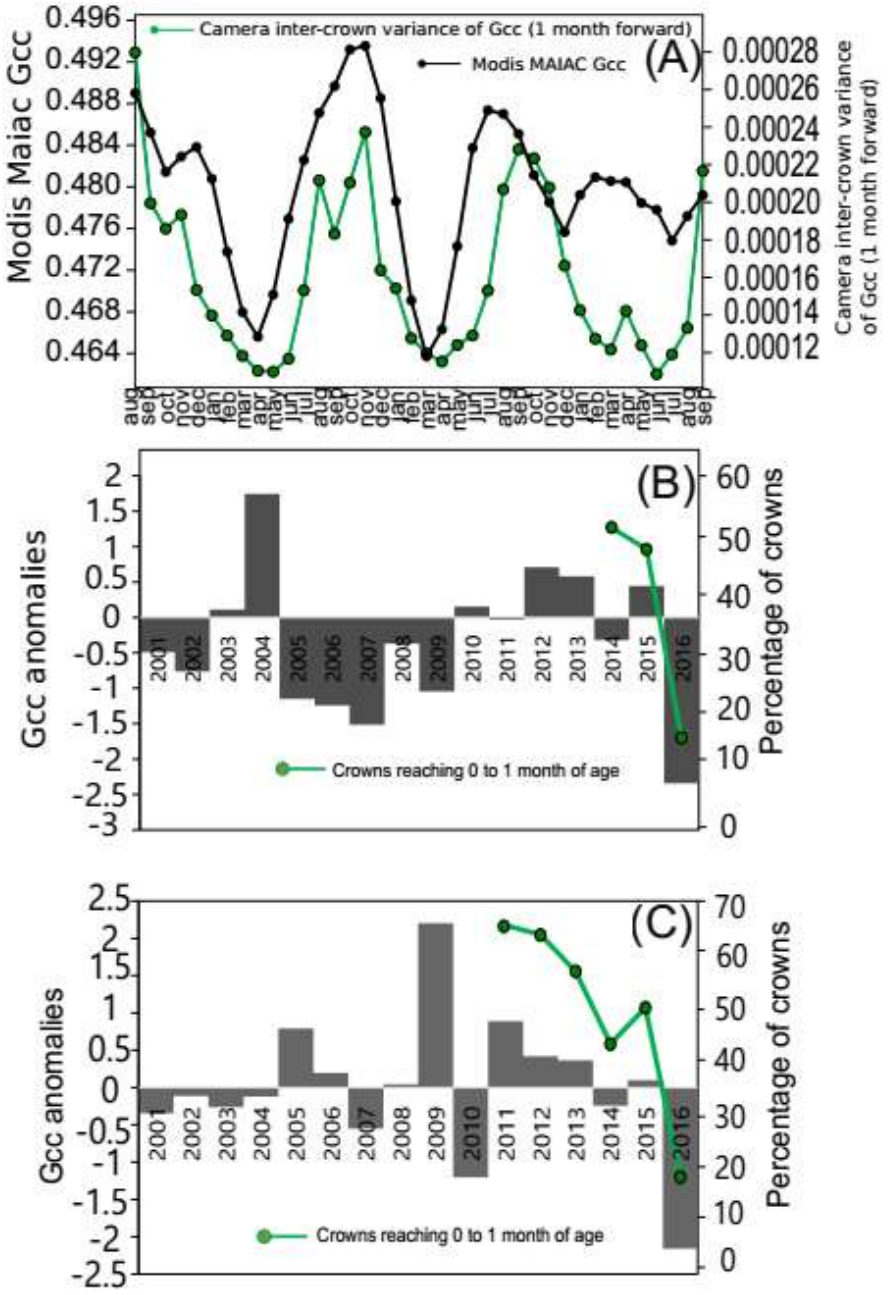

Fig. 6. A) Modis MAIAC Gcc and camera inter-crown variance of Gcc from August 2013 to September 2016 at ATTO. The inter-crown variance of Gcc is shifted one month forward. (B) Anomalies of Modis-MAIAC Gcc for the 16 annual periods of June-July at ATTO tower, plotted against the percentage of recently flushed crowns in this same two-month period, which is when flushing is normally at an annual

peak and (C) same as B, but for Manaus-k34 The “percentage of crowns” that recently flushed is with respect to the total number of crowns that flushed in a year; non-flushing crowns are excluded from the calculation.

DISCUSSION:

Modis MAIAC Gcc and canopy leaf demography

Our first prediction is confirmed: in the Central Amazon, average landscape greenness in the visible portion of the spectrum, as represented by Gcc, is higher in mid dry season (Aug) compared to mid wet season (Feb) for both Landsat 8 and Modis when BRDF artifacts are eliminated. In the continuous Modis data this seasonal contrast is part of a monomodal visible spectrum green-up, with a peak in the early to mid-dry season. This pattern in Gcc is consistent with the RGB camera data and with high resolution QuickBird data. Lopes et al. (2016) found that recently flushed crowns have high Gcc relative to other crown phenostages and that from February towards August there is a large increase in the fraction of upper canopy crowns that have recently flushed out new leaves. In the three months of June to August, close to 40% of all crowns flushed new leaves at their ATTO tower study site, while in the three months of December to February only about 8% of crowns flushed out new leaves. Our results also confirm and extend those of Gonçalves et al. (2016) regarding Gcc seasonality in Landsat 8 OLI.

With the more reliable Landsat 8 OLI data, we have extended to a new and larger area confirmation of dry season green-up across the Central Amazon. Seasonal patterns in Gcc also open a new perspective on leaf phenology and demography patterns detectable with orbital sensors. Gcc and EVI seasonal peaks are four months out of phase, as they are driven by the seasonal abundance of different post-flush crown stages.

EVI and NIR for Modis MAIAC and Landsat 8, when controlling sun-sensor geometry:

We have also confirmed our second prediction – an expected increase of EVI from the Dry-to-Wet transition (May) to the Wet period (December). Landsat 8 OLI for two different scenes now corroborates the seasonal Modis-MAIAC pattern of EVI. However, the seasonal amplitudes were slightly distinct. One possible reason is that we used single date EVI values with Landsat, but seasonal averages and 16 day mosaics for Modis, both of which could cause smoothing. Furthermore, the larger spatial resolution of Modis MAIAC, 1X1 km, could include

some thin clouds and small stream forested floodplains phenologically out of phase with upland forest. With Landsat 30m data we were able to analyze only plateau areas free from clouds and thin clouds.

The values for EVI were different between the two sensors, being consistently higher in Landsat (Fig 2A) than in Modis (Fig 1A) at the same dates. This is expected since Modis MAIAC is generated to emulate a phase angle of 45 degrees while our Landsat 8 scenes compared seasonal pixels having phase angles of about 36 degrees. A larger phase angle increases sub-pixel shade, reducing NIR reflectance, which in turn reduces EVI. Furthermore, there will be more topographic shadows included in the coarser spatial resolution of Modis MAIAC whereas these were eliminated from the 30m Landsat data by masking slopes greater than 4^{o}.

Our second method with near-nadir view and nearly identical solar elevations for the two Landsat dates, also showed strong NIR and EVI seasonality, both increasing from May to December. The NIR increase was large, about 13%. Fully eliminating sun-sensor geometry differences in Landsat seasonal comparisons leaves little doubt about EVI and NIR seasonal green-up and constitutes an independent validation of the BRDF inversion of Modis-MAIAC. Thus, changes in the canopy greenness using EVI are also real and are detectable using medium spatial resolution sensors such as Landsat 8 OLI. These results do not support the conclusions of Morton et al. (2014), of consistent EVI greenness throughout the year.

EVI and canopy leaf demography in the Central Amazon.

Using a fixed sun-sensor geometry (nadir view and 45^{o} solar elevation), to be consistent with Modis-MAIAC, using fixed leaf spectra and using the LAI annual amplitude reported in Wu et al. (2016), of 5.5 to 6.2 m²/m² in K67 site, the ProSail radiative transfer model showed an LAI forcing effect of only 1.4% on EVI. Using the GLAS Lidar-derived LAI amplitude reported in Tang and Dubuyah (2017) for the Central Amazon region – an increase of 0.22 m²/m² from June to October – causes a simulated LAI driven increase of only 1% in EVI (Table 1). These small potential LAI effects on EVIcontrast with the larger (9%) annual amplitude of EVI detected with Modis-MAIAC at the ATTO site. Furthermore, monthly values of upper canopy LAI were a poor predictor of seasonal Modis MAIAC EVI. Canopy LAI thus appears not to be the main driver of change in the remote sensing signal, at least in Central Amazon. Our results strongly suggest that upper canopy leaf age – specifically, the fraction of crowns

having mature leaves 2-7 mo old -- drives the seasonality of EVI signal. Laboratory spectra of tropical forest leaves of know age also show higher NIR reflectance for mature leaves (Roberts et al., 1998; Chavana-Bryant et al., 2016). This study also confirms and extends observations of Lopes et al. (2016) and Wu et al. (2017) about the control of leaf quality over the remote sensing signal.

Table.1 Observed seasonal LAI range, observed seasonal EVI amplitude and ProSail model predicted EVI amplitude driven by LAI alone (using fixed leaf spectra) for the entire Central Amazon region and for three sites within the Central Amazon. Glas Lidar LAI is from Tang and Dubuyah (2017); Km67 LAI is from Wu et al. (2016), K34 and ATTO LAI were estimated from the green crown fraction using equation of Wu et al. (2016).

Site	Observed LAI range (m^2/m^2)	Measured seasonal EVI amplitude	Model predicted EVI amplitude
Glas (Central Amazon region)	4.57 - 4.79	X	1%
Km67 (Tapajós)	5.5 - 6.2	~10%	1.6%
Km34	5.3 - 6.25	~8%	2.4%
ATTO	5.4 - 6.2	~9%	1.9%

Inversion models using only EVI to estimate canopy biophysical parameters (Hilker et al., 2017) should be cautious in this regard. However, another approach to the coupling of LAI using EVI anisotropy (Moura et al., 2015), seems to show sensitivity of EVI to smaller variations in LAI. Furthermore, in others regions of the Amazon with long dry season, where LAI has a broader variation, EVI could be controlled more by total canopy LAI than by leaf demography (Retrepo-Coupe et al 2013).

One factor behind the leaf-age related change in the remote sensing signal of tropical forests is the increase in epiphyll cover. Epiphylls can decrease Near-infrared reflectance (Toomey et al., 2009). Further studies are required to separate the effects of ageing of clean leaves and the increasing epiphyll presence with leaf age (Roberts et al., 1998).

Demography controlling anomalous green-up patterns after 2015-2016 El Niño

We found positive anomalies of EVI in small Modis-MAIC windows over both tower sites in the second trimester (April, May, June) of 2016. Since we show that canopy LAI poorly explains EVI seasonality, this anomalous increase in EVI could only be linked to the maturation of leaves from the anomalous leaf flush that occurred in February and March 2016, as seen in tower camera data for both sites(FIG. 7).

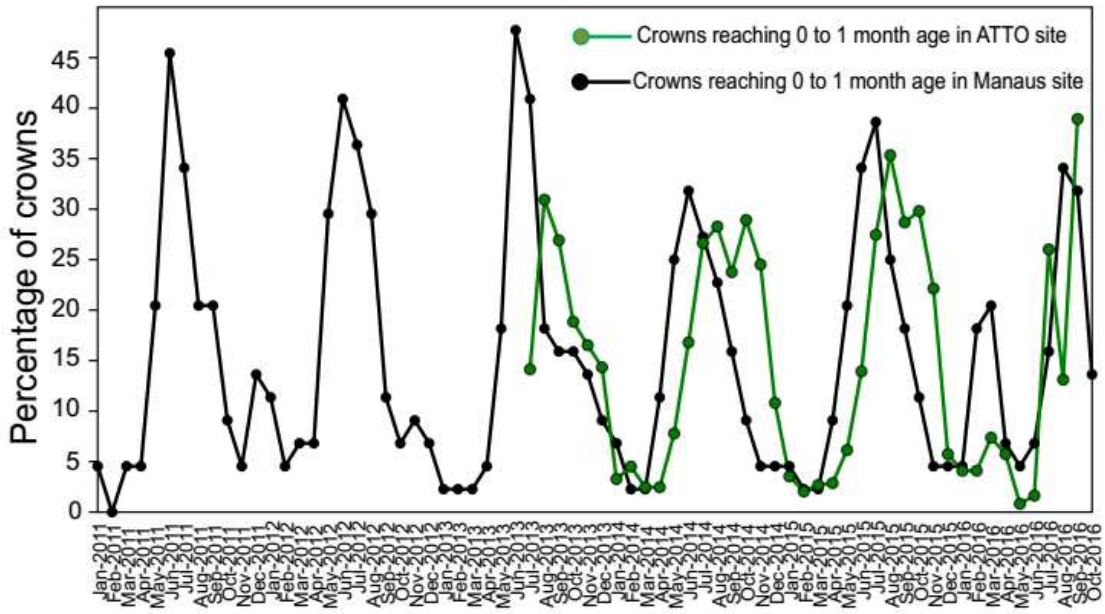

Fig. 7. Percentage of recently flushed crowns (leaf age of 0-1 month) at Manaus k34 and ATTO tower sites. Percentages are with respect to the total number of crowns that flushed sometime during the year at each site. The delay of leaf flush peak at ATTO relative to k34 in normal climate years corresponds to the forward shift of rainfall seasonality as one moves north in the Amazon.

The anomalous leaf flush in the first trimester of 2016 at ATTO and Manaus k34 sites, led to an increase of crowns with mature leaves in the second trimester (Apr-May-Jun), that we infer caused the positive anomalies of Modis-MAIAC EVI during the second trimester. As already shown here, Central Amazon EVI is controlled more by the amount of mature leaves than by the variation in total amount of leaves. Indeed, when analyzing individual leaf spectra as a function of leaf age the reflectance of NIR increases from 0-2 months and remains high until about seven months of age (Roberts et al., 1998; Yang et al., 2014; Chavana-Bryant et al., 2016; Wu et al., 2017). Moreover, tower camera based Gcc (if shifted one month forward) tracks the EVI of Modis MAIAC. Camera Gcc, in its turn, is associated with the bright green

leaf color of newly flushed crowns (Sonnentag et al., 2012; Lopes et al., 2016), showing the control of leaf quality (demography) on the remote sensing signal over evergreen tropical forest canopies.

This concordant seasonality between abundance of recently flushed trees and Modis-MAIAC Gcc, was evident in the long-term mean Modis Gcc seasonality for all pixels within the two Landsat window scenes analyzed. However, the mid-dry season leaf flush signal detected by RGB cameras at both tower sites in normal climate years was not always detected as an increase in the smaller (88 pixel) Modis-MAIAC samples centered on both tower sites. Nonetheless, a negative Gcc anomaly was found for the months of July and August of 2016 in Modis-MAIAC at both towers, when lower-than-normal flush rates also were seen by the cameras. This indicates that the landscape had lower visible greenness in these months, when high rates of leaf exchange would normally take place. The precocious leaf flush that occurred in tower camera data in February/March of 2016 at both sites seems to have also caused the paucity of flushing crowns a few months later, when high rates of flush are normally expected.

When analyzing possible causes of the anomalous precocious flush, we look to the long period of lower-than-normal rainfall that preceded this anomaly at our two tower sites. Rainfall estimates from the 0.25x0.25 degree TRMM 3b43v7 grid cell that includes the Manaus k34 site, show that the five months ending in January of 2016, had the largest accumulated consecutive monthly water deficit ("Maximum Climatological Water Deficit" -- MCWD) for the entire 16y period of TRMM data (Fig. 8). The precocious flush and the subsequent flush deficit were associated with this prolonged and intense drought. El Niño effects on leaf demography seem to be present as a flush deficit five months after the El Niño ended.

This also points out the importance of rainfall -- or of a host of correlated seasonal variables, including herbivore predation pressure on young leaves, young leaf pathogens, poor stomatal control over water loss in old leaves, soil water, vapor pressure deficit, air temperature maxima, PAR, diffuse versus direct fractions of PAR -- as potential triggers or underlying evolutionary drivers (Schaik, Terborgh & Wright, 1993) of the strong seasonality seen in new leaf formation in the Central Amazon. Recent efforts have been made to tease apart the relative contibutions of light and rainfall as cues to new leaf formation across the Amazon (Bi et al. 2015, Wagner et al. 2017).

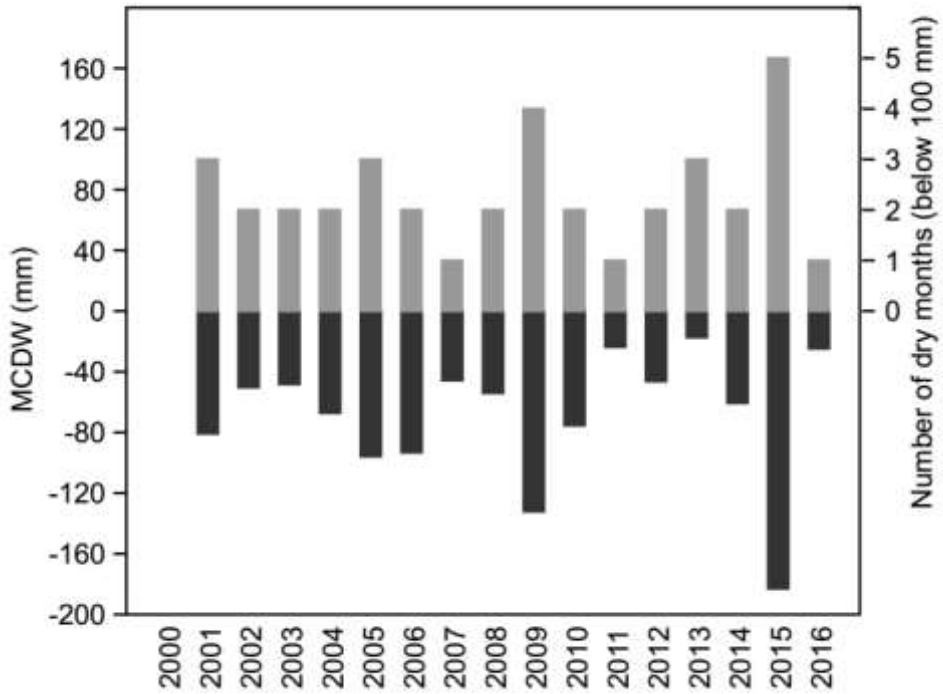

Fig. 8. Maximum climatalogical water deficit (MCWD) and the number of dry months (< 100 mm per month) in each calendar year from 2000 to 2016 at k34 tower site. Both are based on TRMM 3B43v7.

There will be consequences of shifts in leaf phenology after an El Niño event, affecting the timing of the large seasonal changes in intrinsic photosynthetic capacity of the forest and of net primary productivity (Huete et al 2006, Restrepo-Coupe et al 2013, Wu et al 2016) Considering Wu's et al ontogeny model, for instance, the wet season anticipation of flush and the dry season "missing" or delayed flush could make leaves become mature with maximum photosynthetic capacity in an adverse period when environmental variables as temperature, water, and sunlight availability, could limit primary productivity.

CONCLUSIONS:

(1) We validate BRDF corrected Modis EVI seasonality in the Central Amazon with Landsat 8 OLI EVI, obtained under fixed sun-sensor geometry at different seasons;

(2) We extend the Modis-based observations of EVI seasonality in the Central Amazon, including dry season EVI greenup, to two new large areas in the Central Amazon, within two Landsat scenes;

(3) We corroborate at two additional Central Amazon tower sites the recent radiative transfer model-based conclusion of Wu et al (2017) for a single tower site, that LAI is a poor or minor driver of the seasonal change in Central Amazon forest EVI as detected by orbital sensores, while change in leaf spectral quality with age -- mainly the abudance of mature leaves 2-7 mo old -- is a strong driver of seasonal EVI;

(4) Modis Gcc seasonality is consistent with the abundance of the recently flushed (0-1 mo old) age class abundance as detected by tower-mounted RGB cameras; and

(5) Anomalies in leaf demography apparently caused by the 2015/16 El Niño, that were detected by RGB cameras at two tower sites, were also detectable as Modis EVI and Gcc anomalies at both sites.

ACKNOWLEDGEMENTS

We thank the Max Planck Society and Brazil's National Institute for Amazon Research. The Amazon Tall Tower construction, instrumentation and maintenance are supported by the German Federal Ministry of Education and Research (BMBF contract 01LB1001A), the Brazilian Ministry of Science, Technology and Innovation (MCTI/FINEP contract 01.11.01248.00), the Amazonas State University (UEA), FAPEAM, LBA/INPA and SDS/CEUC/RDS-Uatumã. The Amazonas State Foundation for Research Support (FAPEAM) financed the GoAmazon project "Understanding the Response of Photosynthetic Metabolism in Tropical Forests to Seasonal Climate Variations" (PI Marciel José Ferreira).

REFERENCES

Bi, J., Knyazikhin, Y., Choi, S., Park, T., Barichivich, J., Ciais, P., ... Myneni, R. B. (2015). Sun- light mediated seasonality in canopy structure and photosynthetic activity of Amazonian rainforests. *Environmental Research Letters*, 10(6). http://dx.doi.org/10.1088/ 1748-9326/10/6/064014.

Brando, P.M., Goetz, S. J.,Baccini, A., Nepstad, D. C.,Beck, P. S. A.,&Christman, M. C. (2010). Seasonal and interannual variability of climate and vegetation indices across the Amazon. Proceedings of the National Academy of Sciences of the United States of America, 107(33), 14685–14690. http://dx.doi.org/10.1073/pnas. 0908741107.

Conrad, O., Bechtel, B., Bock, M., Dietrich, H., Fischer, E., Gerlitz, L., Wehberg, J., Wichmann, V., and Böhner, J. (2015). System for Automated Geoscientific Analyses (SAGA) v. 2.1.4, *Geoscientific Model Development*,8,1991-2007. http://dx.doi.org/10.5194/gmd-8-1991-2015.

Chavana-Bryant, C., Malhi, Y., Wu, J., Asner, G. P., Anastasiou, A., Enquist, B. J., ... & Martin, R. E. (2017). Leaf aging of Amazonian canopy trees as revealed by spectral and physiochemical measurements. *New Phytologist*, 214(3). http://dx.doi.org/10.1111/nph.13853.

Danaher, T., Wu, X., & Campbell, N. (2001). Bi-directional reflectance distribution function approaches to radiometric calibration of Landsat ETM+ imagery. *Geoscience and Remote Sensing Symposium*, 2001. (Retrieved from:) http://ieeexplore.ieee.org/document/978120/.

Erfanian, A., Wang, G., & Fomenko, L. (2017). Unprecedented drought over tropical South America in 2016: significantly under-predicted by tropical SST. *Scientific reports*, 7(1), 5811. https://dx.doi.org/10.1038%2Fs41598-017-05373-2.

Flood, N. (2013). Testing the local applicability of MODIS BRDF parameters for correcting Landsat TM imagery. *Remote sensing letters*, 4(8), 793-802. https://doi.org/10.1080/2150704X.2013.798709.

Galvão, L.S., Santos, J.R., Roberts, D.A., Breunig, F.M., Toomey, M., Moura, Y.M. (2011). On intra-annual EVI variability in the dry season of tropical forest: A case study with MODIS and hyperspectral data. *Remote Sensing of Environment*, 115,2350-2359. https://doi.org/10.1016/j.rse.2011.04.035.

Galvão, L. S., Breunig, F. M., Teles, T. S., Gaida, W., & Balbinot, R. (2016). Investigation of terrain illumination effects on vegetation indices and VI-derived phenological metrics in subtropical deciduous forests. *GIScience & Remote Sensing*, 53(3), 360-381. https://doi.org/10.1080/15481603.2015.1134140.

Gonçalves, N.B.,Nelson, B. W., Lopes.A.P. (2017). Scaling up canopy leaf phenology in the Central Amazon – from tower mounted RGB cameras to Landsat 8.*Brazilian Symposium of remote sensing*. (Retrieved from:) https://proceedings.galoa.com.br/sbsr/trabalhos/scaling-up-canopy-leaf-phenology-in-the-central-amazon-from-tower-mounted-rgb-cameras-to-landsat-8.

Guan, K., Pan, M., Li, H.,Wolf, A.,Wu, J.,Medvigy, D., ... Lyapustin, A. I. (2015). Photosynthetic seasonality of global tropical forests constrained by hydroclimate. *Nature Geoscience*, 8(4), 284–289.

Hilker, T., Galvão, L. S., Aragão, L. E., de Moura, Y. M., do Amaral, C. H., Lyapustin, A. I., ... & dos Santos, V. A. (2017). Vegetation chlorophyll estimates in the Amazon from multi-angle MODIS observations and canopy reflectance model. *International Journal of Applied Earth Observation and Geoinformation*, 58, 278-287. https://doi.org/10.1016/j.jag.2017.01.014.

Huete, A. R., Didan, K., Shimabukuro, Y. E., Ratana, P., Saleska, S. R.,Hutyra, L. R., &Myneni, R. B. (2006). Amazon rainforests green-up with sunlight in dry season. Geophysical Research Letters, 33(6), L06405. http://dx.doi.org/10.1029/2005GL025583.

Jacquemoud, S., Verhoef, W., Baret, F., Bacour, C., Zarco-Tejada, P. J., Asner, G. P., ... & Ustin, S. L. (2009). PROSPECT+ SAIL models: A review of use for vegetation characterization. *Remote sensing of environment*, 113, S56-S66. https://doi.org/10.1016/j.rse.2008.01.026.

Lopes, A. P., Nelson, B.W., Wu, J., Graça, P. M. L.,Tavares, J. V., Prohaska, N., ... Saleska,S.R.(2016). Leaf flush drives dry season green-up of the Central Amazon. Remote Sensing of Environment, 182: 90-98. https://doi.org/10.1016/j.rse.2016.05.009.

Lyapustin, A. I.,Wang, Y., Laszlo, I., Hilker, T. G., Hall, F., Sellers, P. J., & Korkin, S. V. (2012). Multiangleimplementation of atmospheric correction for MODIS (MAIAC): Atmospheric correction. *Remote Sensing of Environment*, 127,385–393. http://dx.doi.org/10.1016/j.rse.2012.09.002.

Maeda, E. E., & Galvão, L. S. (2015). Sun-sensor geometry effects on vegetation index anomalies in the Amazon rainforest. GIScience & Remote Sensing, 52(3), 332-343. https://doi.org/10.1080/15481603.2015.1038428.

Morton,D.C.,Nagol,J.,Carabajal,C.C.,Rosette,J.,Palace,M.,Cook,B.D., ...North,P.R.J. (2014). Amazon forests maintain consistent canopy structure and greenness during the dry season. *Nature*, 506(7487), 221–224. http://dx.doi.org/10.1038/ nature13006.

Moura, Y. M., Galvão, L. S., Santos, J. R., Roberts, D. A., Breunig, F. M. (2012). Use of MISR/ data to study intra-and inter-annual EVI variations in the dry season of tropical forest. *Remote Sensing of Environment*, 127: 260-270. https://doi.org/10.1016/j.rse.2012.09.013.

Moura, Y. M., Hilker, T., Lyapustin, A. I., Galvão, L. S., Santos, J. R., Anderson, L. O., ... Arai, E. (2015). Seasonality and drought effects of Amazonian forests observed from multi-angle satellite data. *Remote Sensing of Environment*, 171, 278-290. https://doi.org/10.1016/j.rse.2015.10.015.

Moura, Y. M., Galvão, L. S., Hilker, T., Wu, J., Saleska, S., do Amaral, C. H., ... Oliveira, R. C. (2017). Spectral analysis of amazon canopy phenology during the dry season using a tower hyperspectral camera and modis observations. *ISPRS Journal of Photogrammetry and Remote Sensing*, 131, 52-64. https://doi.org/10.1016/j.isprsjprs.2017.07.006.

Nelson, B.W., Tavares, J. V.,Wu, J., Valeriano, D. M., Lopes, A. P.,Marostica, S. F., ...Huete, A. (2014). Seasonality of Central Amazon Forest leaf flush using tower-mounted RGB camera. *American Geophysical Union fall meeting*. (Retrieved from:) https://agu.confex.com/agu/fm14/meetingapp.cgi#Paper/7861.

Ponzoni, F. J., Shimabukuro, Y. E., & Kuplich, T. M. (2007). Sensoriamento remoto no estudo da vegetação (p. 127). São José dos Campos: Parêntese.

R Core Team (2017). R: A language and environment for statistical computing. R Foundation for Statistical Computing, Vienna, Austria. URL: https://www.R-project.org/.

Rennó , C. D., Nobre, A. D., Cuartas, L. A., Soares, J. V., Hodnett, M. G., Tomasella, J., & Waterloo, M. J. (2008). HAND, a new terrain descriptor using SRTM-DEM: Mapping terra-firme rainforest environments in Amazonia. *Remote Sensing of Environment*, 112(9), 3469-3481. https://doi.org/10.1016/j.rse.2008.03.018;

Hijmans, R.J. (2016). raster: Geographic Data Analysis and Modeling. R package version 2.5-8. URL: https://CRAN.R-project.org/package=raster

Roberts, D. A., Nelson, B. W., Adams, J. B., & Palmer, F. (1998). Spectral changes with leaf aging in Amazon caatinga. Trees-Structure and Function, 12(6), 315-325.

Saleska, S. R., Didan, K., Huete, A. R., & da Rocha, H. R. (2007). Amazon forests green-up during 2005 drought. *Science*, 318(5850), 612. http://dx.doi.org/10.1126/science. 1146663.

Saleska, S. R., Wu, J., Guan, K., Restrepo-Coupe, N., Nobre, A. D., Araujo, A., & Huete, A. R. (2016). Dry-season greening of Amazon forests. *Nature Brief Communication Arising*, 531(7594), E4–E5. http://dx.doi.org/10.1038/nature16457.

Samanta, A., Ganguly, S., & Myneni, R. B. (2011).MODIS enhanced vegetation index data do not show greening of Amazon forests during the 2005 drought. New Phytologist, 189(1), 11–15. http://dx.doi.org/10.1111/j.1469-8137.2010.03516.x.

Schaik, C. P., Terborgh, J. W., & Wright, S. J. (1993). The phenology of tropical forests: adaptive significance and consequences for primary consumers. *Annual Review of ecology and Systematics*, *24*(1), 353-377. https://doi.org/10.1146/annurev.es.24.110193.002033.

Solano, R., Didan, K., Jacobson, A., & Huete, A. (2010). MODIS vegetation index user's guide (MOD13 series). Tucson: The University of Arizona 38 pp.

Sonnentag, O., Hufkens, K., Teshera-Sterne, C., Young, A. M., Friedl, M., Braswell, B. H., ... Richardson, A. D. (2012). Digital repeat photography for phenological research in for- est ecosystems. Agricultural and Forest Meteorology, 152,159–177. http://dx.doi.org/ 10.1016/j.agrformet.2011.09.009.

Tang, H., & Dubayah, R. (2017). Light-driven growth in Amazon evergreen forests explained by seasonal variations of vertical canopy structure. *Proceedings of the National Academy of Sciences*, 114(10),2640–2644. http://dx.doi.org/10.1073/pnas.1616943114.

Toomey,M., Roberts, D., & Nelson, B. (2009). The influence of epiphylls on remote sensing of humid forests. *Remote Sensing of Environment*, 113(8), 1787–1798. https://doi.org/10.1016/j.rse.2009.04.002.

Valeriano, D. M., Mello, E. M. K., Moreira, J. C., Shimabukuro, Y. E., Duarte, V., Souza, I. M., ... Souza, R. C. M. (2004). Monitoring tropical forest from space: the PRODES digital project. *International Archives of Photogrammetry Remote Sensing and Spatial Information Sciences*, 35, 272-274.

Xu, L., Samanta, A., Costa, M. H., Ganguly, S., Nemani, R. R., & Myneni, R. B. (2011). Widespread decline in greenness of Amazonian vegetation due to the 2010 drought. Geophysical Research Letters, 38(7). https://doi.org/10.1029/2011GL046824.

Yang, X., Tang, J., &Mustard, J. F. (2014). Beyond leaf color: Comparing camera-based phenologicalmetricswith leaf biochemical, biophysical and spectral properties through- out the growing season of a temperate deciduous forest. *Journal of Geophysical Research – Biogeosciences*, 119(3), 181–191. http://dx.doi.org/10.1002/ 2013JG002460.

Wagner, F. H., Hérault, B., Rossi, V., Hilker, T., Maeda, E. E., Sanchez, A., ... & Aragão, L. E. (2017). Climate drivers of the Amazon forest greening. *PloS one*, 12(7), e0180932. https://doi.org/10.1371/journal.pone.0180932.

Wu, J., Albert, L. P., Lopes, A. P., Restrepo-Coupe, N., Hayek, M., Wiedemann, K. T., ... Saleska, S. R. (2016). Leaf development and demography explain photosynthetic sea- sonality inAmazon evergreen forests. *Science*, 351(6276), 972–976. http://dx.doi.org/ 10.1126/science.aad5068.

Wu, J., Kobayashi, H., Stark, S. C., Meng, R., Guan, K., Tran, N. N., ... & Oliviera, R. C. (2017) . Biological processes dominate seasonality of remotely sensed canopy greenness in an Amazon evergreen forest. *New Phytologist*.217(4),1507-1520. http://dx.doi.org/ 10.1111/nph.14939.

SUPPLEMENTARY DATA

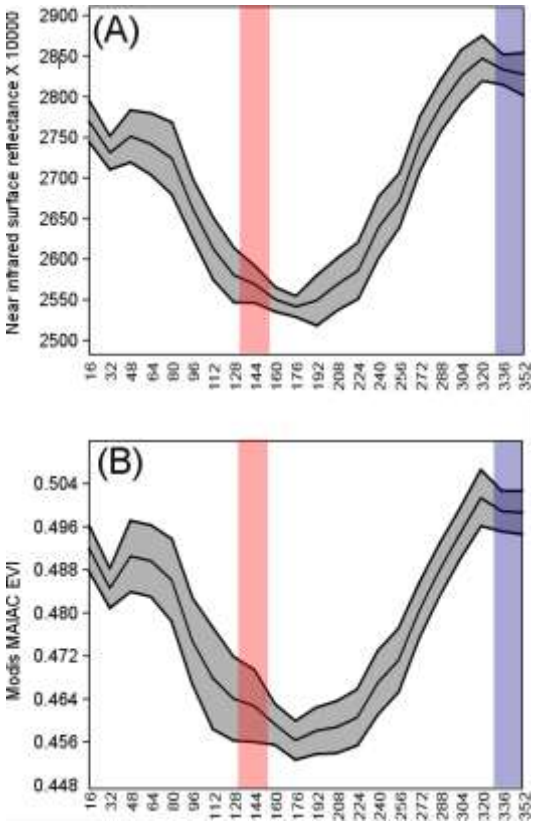

Fig. S1 Sixteen year mean Modis MAIAC EVI (B) and NIR(A) for the upland area of Landsat scene 230/61. The colored strips indicate the three Modis 16d temporal mosaics that correspond to the Landsat image dates used for comparison to Modis. These are blue and red, representing the Wet, Wet-to-Dry transition respectively.

CONCLUSÕES

As medições com o LANDSAT 8 e MODIS MAIAC mostram os mesmos padrões sazonais para Gcc e EVI, quando se controla a geometria de visada e iluminação, confirmando o *green-up* da estação seca. Dessa forma, confirmamos um maior EVI médio para o começo da estação úmida em relação à estação seca e maiores valores médios do índice Gcc (coordenada verde) (Gcc) para estação seca. Além disso mostramos que o Gcc do MODIS MAIAC é controlado pela demografia de foliar (abundância de copas com folhas novas). O EVI, por sua vez, é mais correlacionado com o coorte de folhas maduras do que o LAI (índice de área foliar). Nossos dados, também, sugerem que a seca provocada pelo fenômeno do niño causou desregulações na fenologia foliar de dossel na Amazônia Central, o que explica a forte anomalia positiva do EVI MODIS MAIAC no segundo trimestre de 2016 e uma forte anomalia negativa da Gcc MODIS MAIAC em junho e julho no mesmo ano.

REFERÊNCIAS BIBLIOGRÁFICAS

Bi, J.; Knyazikhin, Y.; Choi, S.; *et al.* 2015. Sun- light mediated seasonality in canopy structure and photosynthetic activity of Amazonian rainforests. *Environmental Research Letters*, 10(6).

Brando, P.M.; Goetz, S. J.;Baccini, A.;Nepstad, D. C.;Beck, P. S. A.;Christman, M. C. 2010. Seasonal and interannual variability of climate and vegetation indices across the Amazon. *Proceedings of the National Academy of Sciences of the United States of America*, 107(33), 14685–14690.

Conrad, O., Bechtel, B., Bock, M.; *et al*.2015. System for Automated Geoscientific Analyses (SAGA) v. 2.1.4, *Geoscientific Model Development*,8,1991-2007.

Chavana-Bryant, C., Malhi, Y., Wu, J.; *et al*. 2017. Leaf aging of Amazonian canopy trees as revealed by spectral and physiochemical measurements. *New Phytologist*, 214(3).

Danaher, T.; Wu, X.; Campbell, N. 2001. Bi-directional reflectance distribution function approaches to radiometric calibration of Landsat ETM+ imagery. *Geoscience and Remote Sensing Symposium*, 2001.

Erfanian, A.; Wang, G.; Fomenko, L. 2017. Unprecedented drought over tropical South America in 2016: significantly under-predicted by tropical SST. *Scientific reports*, 7(1), 5811.

Flood, N. 2013. Testing the local applicability of MODIS BRDF parameters for correcting Landsat TM imagery. Remote sensing letters, 4(8), 793-802.

Galvão, L.S.; Santos, J.R.; Roberts, D.A.; Breunig, F.M.; Toomey, M.; Moura,Y.M. 2011. On intra-annual EVI variability in the dry season of tropical forest: A case study with MODIS and hyperspectral data. Remote Sensing of Environment, 115,2350-2359.

Galvão, L. S.; Breunig, F. M.; Teles, T. S.; Gaida, W.; Balbinot, R. 2016. Investigation of terrain illumination effects on vegetation indices and VI-derived phenological metrics in subtropical deciduous forests. *GIScience & Remote Sensing*, 53(3), 360-381.

Gonçalves, N.B.;Nelson, B. W.; Lopes.A.P. 2017. Scaling up canopy leaf phenology in the Central Amazon – from tower mounted RGB cameras to Landsat 8. Brazilian Symposium of

remote sensing. (Baixado de:) https://proceedings.galoa.com.br/sbsr/trabalhos/scaling-up-canopy-leaf-phenology-in-the-central-amazon-from-tower-mounted-rgb-cameras-to-landsat-8.

Guan, K.; Pan, M.; Li, H.; *et al.* 2015. Photosyn- thetic seasonality of global tropical forests constrained by hydroclimate. *Nature Geoscience*, 8(4), 284–289.

Hilker, T.; Galvão, L. S.; Aragão, L. E.; *et al* 2017. Vegetation chlorophyll estimates in the Amazon from multi-angle MODIS observations and canopy reflectance model. *International Journal of Applied Earth Observation and Geoinformation*, 58, 278-287.

Huete, A. R.; Didan, K.; Shimabukuro, Y. E.; *et al*. 2006. Amazon rainforests green-up with sunlight in dry season. *Geophysical Research Letters*, 33(6), L06405.

Jacquemoud, S.; Verhoef, W.; Baret, F.; *et al.* 2009. PROSPECT+ SAIL models: A review of use for vegetation characterization. Remote sensing of environment, 113, S56-S66.

Lopes, A. P.; Nelson, B.W.; Wu, J. *et al*. 2016. Leaf flush drives dry season green-up of the Central Amazon. Remote Sensing of Environment, 182: 90-98.

Lyapustin, A.; I.,Wang, Y; Laszlo, I.; *et al.* 2012. Multiangleimplementation of atmospheric correction for MODIS (MAIAC): Atmospheric correction. Remote Sensing of Environment, 127,385–393.

Maeda, E. E.;Galvão, L. S. (2015). Sun-sensor geometry effects on vegetation index anomalies in the Amazon rainforest. *GIScience & Remote Sensing*, 52(3), 332-343.

Morton,D.C.;Nagol,J.;Carabajal,C.C.;*et al.* 2014. Amazon forests maintain consistent canopy structure and greenness during the dry season. *Nature*, 506(7487), 221–224.

Moura, Y. M.; Galvão, L. S.; Santos, J. R.; Roberts, D. A.; Breunig, F. M. 2012. Use of MISR/ data to study intra-and inter-annual EVI variations in the dry season of tropical forest. *Remote Sensing of Environment*, 127: 260-270.

Moura, Y. M.; Hilker, T.; Lyapustin, A. I.; *et al.* 2015. Seasonality and drought effects of Amazonian forests observed from multi-angle satellite data. *Remote Sensing of Environment*, 171, 278-290. https://doi.org/10.1016/j.rse.2015.10.015.

Moura, Y. M.; Galvão; L. S., Hilker, T.; *et al.* 2017. Spectral analysis of amazon canopy phenology during the dry season using a tower hyperspectral camera and modis observations. *ISPRS Journal of Photogrammetry and Remote Sensing*, 131, 52-64. https://doi.org/10.1016/j.isprsjprs.2017.07.006.

Nelson, B.W.; Tavares, J. V.; Wu, J. *et al.* 2014. Seasonality of Central Amazon Forest leaf flush using tower-mounted RGB camera. American Geophysical Union fall meeting. (baixado de:) https://agu. confex.com/agu/fm14/meetingapp.cgi#Paper/7861.

Ponzoni, F. J., Shimabukuro, Y. E., & Kuplich, T. M. (2007). Sensoriamento remoto no estudo da vegetação (p. 127). São José dos Campos: Parêntese.

R Core Team.2017. R: A language and environment for statistical computing. R Foundation for Statistical Computing, Vienna, Austria. URL: https://www.R-project.org/.

Rennó, C. D.; Nobre, A. D.; Cuartas, L. A *et al.* 2008. HAND, a new terrain descriptor using SRTM-DEM: Mapping terra-firme rainforest environments in Amazonia. *Remote Sensing of Environment*, 112(9), 3469-3481. https://doi.org/10.1016/j.rse.2008.03.018;

Hijmans, R.J. 2016. raster: Geographic Data Analysis and Modeling. R package version 2.5-8. URL: https://CRAN.R-project.org/package=raster

Roberts, D. A.; Nelson, B. W.;Adams, J. B.;Palmer, F. 1998. Spectral changes with leaf aging in Amazon caatinga. *Trees-Structure and Function*, 12(6), 315-325.

Saleska, S. R.; Didan, K.; Huete, A. R.; da Rocha, H. R. 2007. Amazon forests green-up during 2005 drought. *Science*, 318(5850), 612.

Saleska, S. R.; Wu, J.; Guan, K.; *et al.* 2016. Dry-season greening of Amazon forests. *Nature Brief Communication Arising*, 531(7594), E4–E5.

Samanta, A.; Ganguly, S.; Myneni, R. B. 2011.MODIS enhanced vegetation index data do not show greening of Amazon forests during the 2005 drought. *New Phytologist*, 189(1), 11–15.

Schaik, C. P.; Terborgh, J. W.; Wright, S. J. 1993. The phenology of tropical forests: adaptive significance and consequences for primary consumers. *Annual Review of ecology and Systematics*, *24*(1), 353-377.

Solano, R.; Didan, K.;Jacobson, A.; Huete, A. 2010. MODIS vegetation index user's guide (MOD13 series). Tucson: The University of Arizona 38 pp.

Sonnentag, O., Hufkens, K., Teshera-Sterne, C.; *et al.* 2012. Digital repeat photography for phenological research in for- est ecosystems. *Agricultural and Forest Meteorology*, 152,159–177.

Tang, H.; Dubayah, R. 2017. Light-driven growth in Amazon evergreen forests explained by seasonal variations of vertical canopy structure. *Proceedings of the National Academy of Sciences*, 114(10),2640–2644.

Toomey,M.; Roberts, D.; Nelson, B.W. 2009. The influence of epiphylls on remote sensing of humid forests. *Remote Sensing of Environment*, 113(8), 1787–1798. https://doi.org/10.1016/j.rse.2009.04.002.

Valeriano, D. M.; Mello, E. M. K.; Moreira, J. C.; Shimabukuro, Y. E.; *et al.* 2004. Monitoring tropical forest from space: the PRODES digital project. *International Archives of Photogrammetry Remote Sensing and Spatial Information Sciences*, 35, 272-274.

Xu, L.; Samanta, A.; Costa, M. H.; Ganguly, S.; Nemani, R. R.; Myneni, R. B. 2011. Widespread decline in greenness of Amazonian vegetation due to the 2010 drought. *Geophysical Research Letters*, 38(7). https://doi.org/10.1029/2011GL046824.

Yang, X.; Tang, J.; Mustard, J. F. 2014. Beyond leaf color: Comparing camera-based phe- nologicalmetricswith leaf biochemical, biophysical and spectral properties through- out the growing season of a temperate deciduous forest. *Journal of Geophysical Research – Biogeosciences*, 119(3), 181–191.

Wagner, F. H.; Hérault, B.; Rossi, V.; *et al.* 2017. Climate drivers of the Amazon forest greening. *PloS one*, 12(7), e0180932.

Wu, J.;Albert, L. P.; Lopes, A. P. *et al.* 2016. Leaf development and demography explain photosynthetic sea- sonality inAmazon evergreen forests. *Science*, 351(6276), 972–976.

Wu, J., Kobayashi, H., Stark, S. C.; *et al.* 2017. Biological processes dominate seasonality of remotely sensed canopy greenness in an Amazon evergreen forest. *New Phytologist*.217(4),1507-1520.